



<b>Title</b>	Interactive effect of leaf age and ozone on mesophyll conductance in Siebold's beech
<b>Author(s)</b>	Hoshika, Yasutomo; Haworth, Matthew; Watanabe, Makoto; Koike, Takayoshi
<b>Citation</b>	Physiologia Plantarum, 170(2), 172-186 <a href="https://doi.org/10.1111/ppl.13121">https://doi.org/10.1111/ppl.13121</a>
<b>Issue Date</b>	2020-10
<b>Doc URL</b>	<a href="http://hdl.handle.net/2115/82826">http://hdl.handle.net/2115/82826</a>
<b>Rights</b>	This is the peer reviewed version of the following article: Interactive effect of leaf age and ozone on mesophyll conductance in Siebold's beech, which has been published in final form at 10.1111/ppl.13121. This article may be used for non-commercial purposes in accordance with Wiley Terms and Conditions for Self-Archiving.
<b>Type</b>	article (author version)
<b>File Information</b>	Hoshika et al., 2020_leaf age x O3 on Gm_Physiol Plant.pdf



[Instructions for use](#)

1           **Interactive effect of leaf age and ozone on mesophyll**  
2                           **conductance in Siebold's beech**

3  
4   **Yasutomo Hoshika<sup>1\*</sup>, Matthew Haworth<sup>2</sup>, Makoto Watanabe<sup>3</sup> and Takayoshi**  
5   **Koike<sup>4</sup>**

6  
7   <sup>1</sup>Institute of Research on Terrestrial Ecosystems (IRET), National Research  
8   Council of Italy (CNR), Via Madonna del Piano, I-50019 Sesto Fiorentino, Italy

9   <sup>2</sup>Institute of Sustainable Plant Protection (IPSP), National Research Council of  
10   Italy (CNR), Via Madonna del Piano, I-50019 Sesto Fiorentino, Italy

11   <sup>3</sup>Institute of Agriculture, Tokyo University of Agriculture and Technology, Fuchu  
12   183-8509, Japan

13   <sup>4</sup>Research Faculty of Agriculture, Hokkaido University, Sapporo 060-8689, Japan

14  
15   **Correspondence**

16   \*Corresponding author,  
17   e-mail: yasutomo.hoshika@cnr.it

18  
19   Mesophyll conductance ( $G_m$ ) is one of the most important factors determining  
20   photosynthesis. Tropospheric ozone ( $O_3$ ) is known to accelerate leaf senescence  
21   and causes a decline of photosynthetic activity in leaves. However, the effects of  
22   age-related variation of  $O_3$  on  $G_m$  have not been well investigated, and we,  
23   therefore, analysed leaf gas exchange data in a free-air  $O_3$  exposure experiment on  
24   Siebold's beech with two levels (ambient and elevated  $O_3$ : 28 and 62  $nmol\ mol^{-1}$   
25   as daylight average, respectively). In addition, we examined whether  $O_3$ -induced  
26   changes on leaf morphology (leaf mass per area, leaf density and leaf thickness)

27 may affect CO<sub>2</sub> diffusion inside leaves. We found that O<sub>3</sub> damaged the  
 28 photosynthetic biochemistry progressively during the growing season. The  $G_m$  was  
 29 associated with a reduced photosynthesis in O<sub>3</sub>-fumigated Siebold's beech in  
 30 August. The O<sub>3</sub>-induced reduction of  $G_m$  was negatively correlated with leaf  
 31 density, which was increased by elevated O<sub>3</sub>, suggesting that the reduction of  $G_m$   
 32 was accompanied by changes in the physical structure of mesophyll cells. On the  
 33 other hand, in October, the O<sub>3</sub>-induced decrease of  $G_m$  was diminished because  $G_m$   
 34 decreased due to leaf senescence regardless of O<sub>3</sub> treatment. The reduction of  
 35 photosynthesis in senescent leaves after O<sub>3</sub> exposure was mainly due to a decrease  
 36 of maximum carboxylation rate ( $V_{cmax}$ ) and/or maximum electron transport rate  
 37 ( $J_{max}$ ) rather than diffusive limitations to CO<sub>2</sub> transport such as  $G_m$ . A leaf age×O<sub>3</sub>  
 38 interaction of photosynthetic response will be a key for modelling photosynthesis  
 39 in O<sub>3</sub>-polluted environments.

40

41 *Abbreviations*

42	$C_c$	CO <sub>2</sub> concentration inside the chloroplast envelope ( $\mu\text{mol mol}^{-1}$ )
43	$C_i$	Sub-stomatal CO <sub>2</sub> concentration ( $\mu\text{mol mol}^{-1}$ )
44	ETR	Rate of electron transport ( $\mu\text{mol m}^{-2} \text{s}^{-1}$ )
45	$\Phi$	Initial slope of photosynthetic light response curve ( $\text{mol mol}^{-1}$ )
46	$\Phi_{CO_2}$	Quantum efficiency of carbon gain (dimensionless)
47	$\Phi_{PSII}$	Quantum yield of PSII in the light (dimensionless)
48	$\Gamma$	Light compensation point ( $\mu\text{mol mol}^{-1}$ )
49	$\Gamma^*$	CO <sub>2</sub> compensation point to photorespiration ( $\mu\text{mol mol}^{-1}$ )
50	$G_m$	Mesophyll conductance to CO <sub>2</sub> ( $\text{mol m}^{-2} \text{s}^{-1} \text{bar}^{-1}$ )
51	$G_{sCO_2}$	Stomatal conductance for CO <sub>2</sub> ( $\text{mol m}^{-2} \text{s}^{-1}$ )
52	$G_{sH_2O}$	Stomatal conductance for water vapour ( $\text{mol m}^{-2} \text{s}^{-1}$ )

53	$G_{\text{totCO}_2}$	Total conductance to $\text{CO}_2$ ( $\text{mol m}^{-2} \text{s}^{-1}$ )
54	$J_{\text{max}}$	Maximum rate of electron transport required for RuBP regeneration ( $\mu\text{mol}$
55		$\text{m}^{-2} \text{s}^{-1}$ )
56	$l_b$	Relative biochemical limitation to photosynthesis (%)
57	LD	Leaf density ( $\text{g cm}^{-3}$ )
58	$l_b$	Relative mesophyll conductance limitation to photosynthesis (%)
59	LMA	Leaf mass per area ( $\text{g cm}^{-2}$ )
60	$l_b$	Relative stomatal limitation to photosynthesis (%)
61	LT	Leaf thickness (mm)
62	$P_N$	Net photosynthetic rate ( $\mu\text{mol m}^{-2} \text{s}^{-1}$ )
63	$P_{N\text{sat}}$	Light-saturated net photosynthetic rate ( $\mu\text{mol m}^{-2} \text{s}^{-1}$ )
64	$R_d$	Respiration in the light ( $\mu\text{mol m}^{-2} \text{s}^{-1}$ )
65	$R_n$	Respiration in the dark ( $\mu\text{mol m}^{-2} \text{s}^{-1}$ )
66	$R_{\text{PR}}$	Photorespiration ( $\mu\text{mol m}^{-2} \text{s}^{-1}$ )
67	$V_{\text{cmax}}$	Maximum rate of RuBP carboxylation ( $\mu\text{mol m}^{-2} \text{s}^{-1}$ )
68		
69		
70		
71		
72		
73		
74		
75		
76		
77		
78		

## 79 **Introduction**

80 Anthropogenic emissions of air pollutants such as nitrogen oxides (NO<sub>x</sub>) and  
81 volatile organic compounds have elevated the ground-level concentration of ozone  
82 (O<sub>3</sub>) since pre-industrial times (Mills et al. 2018). Ozone is phytotoxic to plants,  
83 adversely affecting physiological and biochemical processes contributing to a  
84 decline in plant growth (Matyssek et al. 2013, Grulke and Heath 2020).

85 In cool-temperate forests in Japan, deciduous broadleaved Siebold's beech  
86 (*Fagus crenata*) is the dominant tree species (Koike et al. 1998). Previous  
87 experimental studies have shown that Siebold's beech is highly sensitive to O<sub>3</sub> (e.g.  
88 Yamaguchi et al. 2011, Izuta 2017). Watanabe et al. (2012) estimated that the  
89 current concentration of O<sub>3</sub> in Japan may reduce the growth of Siebold's beech  
90 from 3.2% to a maximum of 9.7%. This O<sub>3</sub> induced reduction in tree growth is  
91 considered to be related to lower photosynthetic activity (Watanabe et al. 2014a).  
92 The exact mechanisms underlying the effects of O<sub>3</sub> on photosynthesis are still  
93 unclear. However, previous studies have suggested that O<sub>3</sub> causes biochemical  
94 limitations associated with reduced ribulose-1,5-bisphosphate  
95 carboxylase/oxygenase (Rubisco) activity in leaves (Fiscus et al. 2005, Hoshika et  
96 al. 2013, Watanabe et al. 2014a, 2014b, Bagard et al. 2015). The loss of Rubisco  
97 activity is commonly inferred from decreases in the maximum rate of carboxylation  
98 ( $V_{cmax}$ ), as indicated by a decrease in the initial slope of a  $P_N/C_i$  curve (net  
99 photosynthetic rate versus estimated sub-stomatal CO<sub>2</sub> concentration; e.g.  
100 Matyssek et al. 2012, Watanabe et al. 2013). Any loss in the biochemical efficiency  
101 of CO<sub>2</sub> assimilation induced by O<sub>3</sub> exposure may also be evident in a decline in the  
102 maximum rate of electron transport required for ribulose-1,5-bisphosphate (RuBP)  
103 regeneration ( $J_{max}$ ; Hoshika et al. 2013). The traditional calculation of  
104 photosynthetic parameters from  $P_N/C_i$  curves assumes an infinite mesophyll

105 conductance to CO<sub>2</sub> ( $G_m$ ; e.g. Long and Bernacchi 2003). However,  $G_m$  may exert  
106 similar limits to  $P_N$  as stomatal resistance to CO<sub>2</sub> transport (Terashima et al. 1995,  
107 Lauteri et al. 2014, Killi and Haworth 2017, Gago et al. 2019, Veromann-Jürgenson  
108 et al. 2020). This indicates that previous observations of the O<sub>3</sub>-induced reduction  
109 of  $V_{cmax}$  and  $J_{max}$  parameters calculated from  $P_N/C_i$  curves assuming infinite  $G_m$   
110 incorporate not only biochemical limitations but also the effect of  $G_m$  (Warren et  
111 al. 2007).

112 The generation of reactive oxygen species during O<sub>3</sub> exposure could disrupt the  
113 physical integrity and biochemistry of mesophyll cells (Kangasjärvi et al. 2005).  
114 This would suggest that the exposure to O<sub>3</sub> would impair both the physical and  
115 biochemical transport of CO<sub>2</sub> from the sub-stomatal leaf air-space to chloroplasts.  
116 In fact, a reduction in  $G_m$  was observed in O<sub>3</sub>-sensitive snapbean (*Phaseolus*  
117 *vulgaris*) exposed to 60 nmol mol<sup>-1</sup> O<sub>3</sub>, while no effect was observed on the  $G_m$   
118 values of resistant varieties (Flowers et al. 2007). Xu et al. (2019) found that the  
119 O<sub>3</sub>-induced reduction of photosynthesis was mainly due to a decreased  $G_m$  in a  
120 hybrid poplar clone. In addition, Watanabe et al. (2018a) reported that O<sub>3</sub> exposure  
121 reduced  $G_m$  in Siebold's beech without any effect on  $C_c$ -based  $V_{cmax}$ . However,  
122 European beech (*F. sylvatica*) grown in an O<sub>3</sub> FACE system showed no effect of a  
123 doubling of ambient O<sub>3</sub> concentration on  $G_m$  (Warren et al. 2007). Likewise,  
124 fumigation of localized areas of Holm oak (*Quercus ilex*) and pubescent oak (*Q.*  
125 *pubescens*) leaves with O<sub>3</sub> between 50 to 350 nmol mol<sup>-1</sup> did not reduce  $G_m$   
126 (Velikova et al. 2005).

127 Mesophyll conductance is generally lower in leaves with thicker cell walls and  
128 greater leaf density (Adachi et al. 2013, Ivanova et al. 2018) that are conditions  
129 limiting the diffusion of CO<sub>2</sub> in the leaf liquid phase (Tomás et al. 2013, Onoda et  
130 al. 2017). Ozone may affect leaf morphology, which is likely to modify the CO<sub>2</sub>

131 diffusion inside leaves (Heath 1994, Moura et al. 2018). The white poplar (*Populus*  
132 *alba*) grown in an O<sub>3</sub>-enriched atmosphere (150 nmol mol<sup>-1</sup>) developed thicker and  
133 denser leaves than that grown in clean air (Fares et al. 2006). Likewise, leaf density  
134 (LD) was increased by O<sub>3</sub> in European silver birch (*Betula pendula*; Oksanen 2005)  
135 and European beech (Bussotti et al. 2005). In contrast, the leaves of Pima cotton  
136 (*Gossypium barbadense*) formed in O<sub>3</sub>-enriched air showed lower mesophyll  
137 density (Grantz and Shrestha 2006), probably due to damage and disruption of the  
138 mesophyll cells (Günthardt-Goerg et al. 1993). Watanabe et al. (2018a) did not find  
139 any effect of O<sub>3</sub> on leaf morphology in Siebold's beech, although plants were  
140 exposed to relatively low O<sub>3</sub> concentrations (29 to 47 nmol mol<sup>-1</sup> as daylight  
141 average). The density of cells in the mesophyll layer is closely related to leaf mass  
142 per area (LMA; Haworth and Raschi 2014). Meta-analysis suggests that the effect  
143 of O<sub>3</sub> on LMA is not pronounced or uni-directional (Poorter et al. 2009), raising  
144 the likelihood that O<sub>3</sub> effects on leaf structure depend on species or varieties  
145 (Pääkkönen et al. 1995).

146 Previous works have shown that  $G_m$  is variable with leaf age (Loreto et al. 1994,  
147 Niinemets et al. 2009, Tosens et al. 2012, Marino et al. 2020). After the onset of  
148 leaf senescence,  $G_m$  reduced due to age-dependent variation of leaf structure and  
149 physiological activity (Niinemets et al. 2009). It is known that leaf senescence is  
150 accelerated by O<sub>3</sub> (Grulke and Heath 2020). As a matter of fact, O<sub>3</sub>-induced  
151 structural changes in chloroplasts appear to be similar to those during autumn  
152 senescence (e.g. Vollenweider et al. 2019), which may be associated with a reduced  
153 mesophyll CO<sub>2</sub> diffusion. The question was therefore raised if O<sub>3</sub> and leaf age  
154 could interactively affect  $G_m$ , but the age-related change of O<sub>3</sub> effect on  $G_m$  has  
155 not been addressed in previous studies.

156 To examine a leaf age×O<sub>3</sub> interaction on  $G_m$ , we measured leaf gas exchange

157 three times (June, August, October) in a free-air O<sub>3</sub> exposure experiment on  
158 Siebold's beech. The aim of the present study was to: (1) characterise the effect of  
159 O<sub>3</sub> fumigation on diffusive resistances to P<sub>N</sub>, in particular the impact on G<sub>m</sub> values  
160 derived from the variable J method (Harley et al. 1992, Loreto et al. 1992), while  
161 comparing with those derived from the P<sub>N</sub>/C<sub>i</sub> curve fitting approach (Ethier and  
162 Livingston 2004); (2) assess the impact of O<sub>3</sub> exposure on the efficiency of  
163 photosynthetic light capture; and (3) analyse the interaction between O<sub>3</sub> fumigation  
164 and leaf morphology (LMA, LD and leaf thickness), and the impact upon  
165 photosynthetic physiology throughout the growing season.

166

## 167 **Materials and Methods**

### 168 **Experimental site and plant material**

169 Measurements were conducted at a free-air O<sub>3</sub> exposure experiment facility located  
170 in the Sapporo Experimental Forest, Hokkaido University, in northern Japan  
171 (43°04' N, 141°20' E, 15 m a.s.l., mean annual temperature: 8.9°C, mean total  
172 annual precipitation: 1107 mm, the snow-free period was late April to mid-  
173 November). The details of the system are described in Watanabe et al. (2013). The  
174 soil is a brown forest soil (Dystric Cambisols). Two plots were established, one for  
175 ambient O<sub>3</sub> (AA) and the other for elevated O<sub>3</sub> (eO<sub>3</sub>). The size of each plot was 5.5  
176 m × 7.2 m. The distance between the O<sub>3</sub>-enhanced plot and the ambient plot was  
177 about 20 m, which was enough distance for the O<sub>3</sub>-enriched air not to affect the  
178 AA plot (Watanabe et al. 2013). Ten seedlings of two-year-old Siebold's beech  
179 (*Fagus crenata*) were obtained from a nearby nursery and planted in each plot in  
180 May 2003 and then grown under ambient conditions from 2003 to 2010. The plants  
181 were ten years old and well-established when fumigation with O<sub>3</sub> began in 2011.  
182 The 11-year-old Siebold's beech saplings analysed in this study were around 3.4  
183 m in height in 2012. We confirmed that photosynthetic parameters, plant height  
184 and diameter were not different between treatments before O<sub>3</sub> exposure (in July  
185 2011, data not shown). The target O<sub>3</sub> concentration was 60 nmol mol<sup>-1</sup> during  
186 daylight hours. The enhanced O<sub>3</sub> treatment was employed during daylight hours to

187 ten Siebold's beech saplings from August to November in 2011, and from May to  
188 November in 2012. Ozone concentrations at canopy height were recorded  
189 continuously by an O<sub>3</sub> monitor (Mod. 202, 2B Technologies). The daytime hourly  
190 mean of O<sub>3</sub> concentration in AA and eO<sub>3</sub> were 28 nmol mol<sup>-1</sup> and 62 nmol mol<sup>-1</sup>,  
191 respectively, during the 2012 experimental period. The level of O<sub>3</sub> concentration  
192 in eO<sub>3</sub> was equal to the environmental standard value in Japan (= 60 nmol mol<sup>-1</sup>),  
193 and has been frequently observed in many Asian regions including forested areas  
194 (Izuta 2017). The soil moisture was measured in the root layer (at depth 20 cm) by  
195 10HS sensors equipped with an EM5b data logger (Decagon Devices). The average  
196 soil moisture (volumetric soil water content) was  $28.1 \pm 2.8\%$  during these  
197 measurements. These values were equivalent to the field capacity of the soil.  
198 Previous studies have established that no reduction in  $P_N$  due to soil water content  
199 occurred during the growing season for Siebold's beech in this experiment  
200 (Hoshika et al. 2012, 2013, Watanabe et al. 2014a).

201

## 202 **Measurement of leaf gas exchange**

203 Leaf gas exchange was measured in fully expanded leaves exposed to full sun at  
204 the top of the canopy ( $n = 6$  trees in each O<sub>3</sub> treatment) using a Li6400 portable  
205 infra-red gas analyzer (Li-Cor instruments). Only first flush leaves (flushed in  
206 May) were used for these measurements, because the number of second flush leaves  
207 was very small (0.16% of the total leaf number taken over all saplings).  
208 Measurements were undertaken on 15-16 June, 26-31 August and 9-16 October on  
209 days with clear sky between 8:00 and 16:00 h. Conditions within the leaf cuvette  
210 were set to maintain a leaf temperature of 25°C and the leaf-to-air vapour pressure  
211 deficit (VPD) within a range of 1.0-1.8 kPa. The Li6400 was connected to a 6400-  
212 40 leaf chamber fluorimeter cuvette with red and blue LEDs when conducting the  
213  $P_N$  – photosynthetic photon flux density (PPFD) response curves. The response of  
214  $P_N$  to PPFD was measured at 11 light intensities (1500, 1100, 800, 500, 400, 300,  
215 200, 100, 75, 50, 0  $\mu\text{mol m}^{-2} \text{s}^{-1}$ ). At each stage of the  $P_N$ /PPFD curve,  $P_N$ , stomatal  
216 conductance ( $G_{\text{sH}_2\text{O}}$ ), and the quantum yield of PSII in the light ( $\Phi_{\text{PSII}}$ ) were  
217 recorded. The  $P_N$ /PPFD response curves were utilised to calculate the light  
218 saturated rate of  $P_N$  ( $P_{N\text{sat}}$ ), initial slope of photosynthetic light response curve ( $\Phi$ ),  
219 light compensation point ( $\Gamma$ ) and the quantum efficiency of carbon gain ( $\Phi_{\text{CO}_2}$ )  
220 following Kaipiainen et al. (2009). The Kok (1948) method was used to estimate

221 respiration in the light ( $R_d$ ). The effect of variation in the sub-stomatal  
 222 concentration of [ $\text{CO}_2$ ] ( $C_i$ ) on  $R_d$  was corrected using the iterative method of  
 223 Kirschbaum and Farquhar (1987). Respiration in the dark ( $R_n$ ) was measured by  
 224 switching off the LED light unit after the Kok protocol, shading the area of the  
 225 plant being measured and recording the rate of  $\text{CO}_2$  efflux from the leaf, after  
 226 values had remained stable for 5-10 min. Mesophyll conductance was calculated at  
 227  $P_{N_{\text{sat}}}$  using the variable J method as described by Loreto et al. (1992):

$$228 \quad G_m = \frac{P_{N_{\text{sat}}}}{C_i - \frac{\Gamma^* \cdot [ETR + 8 \cdot (P_N + R_d)]}{ETR - 4 \cdot (P_N + R_d)}} \quad (1),$$

230  
 231 where the electron transport rate (ETR) is calculated from fluorescence (Genty et  
 232 al. 1989) as following:

$$233 \quad ETR = \text{PPFD} \cdot \varphi\text{PSII} \cdot \alpha \cdot \beta \quad (2),$$

234  
 235 where the partitioning factor ( $\beta$ ) between photosystems I and II was considered to  
 236 be 0.5 and leaf absorbance ( $\alpha = 0.85$ ; Laik and Loreto 1996). The  $\text{CO}_2$   
 237 compensation point to photorespiration ( $\Gamma^*$ ) was calculated using the Rubisco  
 238 specificity factor of Galmes et al. (2005). Total conductance to  $\text{CO}_2$  ( $G_{\text{totCO}_2}$ ) was  
 239 calculated as:

$$240 \quad G_{\text{totCO}_2} = [G_{\text{sCO}_2} \cdot G_m] / [G_{\text{sCO}_2} + G_m] \quad (3).$$

241  
 242 where  $G_{\text{sCO}_2}$  is the stomatal conductance for  $\text{CO}_2$ . The concentration of [ $\text{CO}_2$ ] inside  
 243 the chloroplast envelope ( $C_c$ ) was calculated using the value of  $G_m$  produced by the  
 244 variable J method as:

$$245 \quad C_c = C_i - \frac{P_{N_{\text{sat}}}}{G_m} \quad (4).$$

246  
 247 Photorespiration ( $R_{\text{PR}}$ ) was determined following Sharkey (1988):

$$248 \quad R_{\text{PR}} = \frac{P_{N_{\text{sat}}} + R_d}{\frac{C_c}{\Gamma^*} - 1} \quad (5).$$

254

255 Hoshika et al. (2013) previously reported the  $P_N/C_i$  curves of the Siebold's beech  
 256 exposed to O<sub>3</sub>-FACE, based on the approach by Long and Bernacchi (2003) that  
 257 assumed infinite  $G_m$ . Here the  $P_N/C_i$  data were re-analysed using the protocol of  
 258 Ethier and Livingston (2004) to consider  $G_m$  values using the curve-fitting  
 259 approach. The  $P_N/C_i$  curves were obtained by measuring  $P_N$  over 12 [CO<sub>2</sub>] steps  
 260 ( $C_a$ , 380, 300, 220, 140, 60, 300, 380, 500, 800, 1100, 1400, 1700  $\mu\text{mol mol}^{-1}$ ). The  
 261 response of  $P_N$  to  $C_i$  was then used to calculate the carboxylation capacity of  
 262 ribulose-1,5-bisphosphate carboxylase/ oxygenase (Rubisco;  $V_{c\text{max}}$ ) and the  
 263 maximum rate of electron transport required for ribulose-1,5-bisphosphate (RuBP)  
 264 regeneration ( $J_{\text{max}}$ ), assuming that  $G_m$  were constant at all [CO<sub>2</sub>] steps. All gas  
 265 exchange data were corrected for leaks from gaskets using an empty cuvette and  
 266 the entire chamber head was enclosed in a plastic bag to minimise the effect of  
 267 leak (Flexas et al. 2007).

268 According to Grassi and Magnani (2005), the relative limitations in  $P_{N\text{sat}}$   
 269 (stomatal limitation,  $l_s$ ; mesophyll conductance limitation,  $l_m$ ; biochemical  
 270 limitation,  $l_b$ ) were determined as follows:

271

$$272 \quad l_s = \frac{G_{\text{totCO}_2}/G_{s\text{CO}_2} \cdot \delta P_{N\text{sat}}/\delta C_c}{G_{\text{totCO}_2} + \delta P_{N\text{sat}}/\delta C_c} \quad (6),$$

273

$$274 \quad l_m = \frac{G_{\text{totCO}_2}/G_m \cdot \delta P_{N\text{sat}}/\delta C_c}{G_{\text{totCO}_2} + \delta P_{N\text{sat}}/\delta C_c} \quad (7),$$

275

$$276 \quad l_b = \frac{G_{\text{totCO}_2}}{G_{\text{totCO}_2} + \delta P_{N\text{sat}}/\delta C_c} \quad (8),$$

277

278 where  $\delta P_{N\text{sat}}/\delta C_c$  is an initial slope of  $P_N/C_c$  curves ( $C_c$ : over a range of 0–150  $\mu\text{mol}$   
 279  $\text{mol}^{-1}$ ).

280

### 281 **Measurements of leaf traits**

282 After the measurement of gas exchange rate, leaves were collected for the  
 283 determination of the leaf mass per unit area (LMA), leaf density (LD) and leaf  
 284 thickness (LT). LT was measured avoiding the mid-vein by using a hand-held  
 285 micrometer (Digimatic micrometer, Mitsutoyo). The projected area (one side of the  
 286 leaf) was determined with image-processing software (LIA 32, Nagoya University,

287 Japan). Leaves were then dried in an oven at 70°C for 1 week and were then  
288 weighed. The LMA was calculated as the ratio of the dry mass to the area of the  
289 leaves. The LD was calculated as the leaf dry mass per unit leaf volume.

290

## 291 **Data analysis**

292 Statistical analyses were performed using R 3.5.1 (R Core Team 2018). To test the  
293 effects of O<sub>3</sub> fumigation treatment and measurement months, a two-way ANOVA  
294 was used to assess differences in variance between samples. Linear regression was  
295 used to investigate possible relationships between  $P_N$  and diffusive limitations to  
296 CO<sub>2</sub> transport and leaf traits. For these analyses, we used  $G_m$  values derived from  
297 variable J method. Principle component analysis (PCA) was used to investigate  
298 patterns in the photosynthetic capacity, light harvesting and diffusive components  
299 of photosynthesis in Siebold's beech after fumigation with O<sub>3</sub>. Results were  
300 considered significant at  $P < 0.05$ .

301

## 302 **Results**

### 303 **Leaf density is modulated by ozone and season**

304 No significant effects of O<sub>3</sub> or measurement month on LMA and LT were found  
305 (Table 1). On the other hand, LD was significantly increased by O<sub>3</sub>. In addition,  
306 LD increased with season as it was relatively smaller in June (0.45 g cm<sup>-3</sup> in AA  
307 and 0.44 g cm<sup>-3</sup> in eO<sub>3</sub>) compared to in October (0.48 g cm<sup>-3</sup> in AA and 0.54 g cm<sup>-3</sup>  
308 in eO<sub>3</sub>).

309

### 310 **Photosynthetic parameters are progressively decreased by ozone**

311 Most photosynthetic parameters of Siebold's beech were significantly affected by  
312 O<sub>3</sub> exposure (Fig. 1, Table 2). Ozone decreased  $P_{Nsat}$  of Siebold beech trees in

313 August (-28%) and October (-46%), although  $P_{N_{\text{sat}}}$  values in both  $O_3$  treatments  
314 were similar in June (-7% in  $eO_3$  compared to in AA; Fig. 1A). Significant  
315 increases of  $R_n$  were induced by  $O_3$  (+70% in August and +88% in October; Fig.  
316 1B). There were no significant changes in  $R_{PR}$  associated with elevated  $O_3$  in either  
317 June or August (Fig. 1C). However,  $O_3$  decreased  $R_{PR}$  by 56% relative to AA plants  
318 in October. Ozone decreased  $G_{sH_2O}$ ,  $G_m$  and  $G_{\text{totCO}_2}$ , although significant differences  
319 were not observed between the treatments in October (Fig. 1D-F). In addition, the  
320 measurements by fluorimeter indicated that the PSII electron transport rate (ETR)  
321 and actual quantum efficiencies of PSII ( $\Phi_{PSII}$ ) were significantly decreased by  
322  $O_3$  (Table 2, Fig. 2H,L). The  $eO_3$  treatment significantly reduced  $P_{N_{\text{sat}}}$  and values  
323 of  $V_{c_{\text{max}}}$  and  $J_{\text{max}}$  from the  $P_N/C_c$  curves (Table 2, Fig. S1). A significant increase  
324 in the  $J_{\text{max}}/V_{c_{\text{max}}}$  ratio was found in October due to a larger reduction in  $V_{c_{\text{max}}}$  than  
325  $J_{\text{max}}$  after  $O_3$  exposure. Estimated values of  $G_m$  derived from the  $P_N/C_i$  response  
326 curves approach were matched with those calculated by the variable J method (Fig.  
327 S2).

328 Rates of  $P_{N_{\text{sat}}}$  were positively correlated to the measures of  $CO_2$  conductance  
329 under AA conditions (Fig. 3A-C). However, in  $eO_3$ ,  $P_{N_{\text{sat}}}$  was not associated with  
330  $G_{sH_2O}$  (Fig. 3A). In addition, no significant relationship between  $G_m$  and  $G_{sH_2O}$  was  
331 found in  $eO_3$  (Fig. 3D).

332 The light-saturated net photosynthetic rate ( $P_{N_{\text{sat}}}$ ) and diffusive conductance  
333 parameters ( $G_{sH_2O}$ ,  $G_m$  and  $G_{\text{totCO}_2}$ ) were not correlated with LD under the AA  
334 condition (Fig. 4A-D). On the other hand, in  $eO_3$ ,  $P_{N_{\text{sat}}}$ ,  $G_m$  and  $G_{\text{totCO}_2}$  showed  
335 negative relationships with LD (Fig. 4A,C,D), while there was no significant  
336 correlation between LD and  $G_{sH_2O}$  (Fig. 4B). LMA and LT did not correlate to those  
337 diffusive conductance parameters in both  $O_3$  treatments (Figs S3 and S4).

338

**339 Relative limitations to photosynthesis are affected by ozone and season**

340 The relative limitations to photosynthesis ( $l_s$ ,  $l_m$  and  $l_b$ ) are shown in Table 3.  
341 Relative limitation to photosynthesis by stomata ( $l_s$ ) decreased with season. In  
342 particular, in eO<sub>3</sub>, the reduction in  $l_s$  was remarkable in the end of the growing  
343 season ( $l_s$ : -39% in August, -54% in October compared to June). On the other hand,  
344 the  $l_b$  increased over the season, and this was highlighted in eO<sub>3</sub> according to the  
345 post-hoc Tukey test. A relative limitation to photosynthesis by mesophyll  
346 conductance ( $l_m$ ) was rather constant among the sampling campaigns  
347 (approximately 30 to 40% over the season).

348

**349 Principal component analysis revealed the interaction of leaf age and ozone on  
350 photosynthetic response**

351 Principal component analysis of parameters derived from analyses of the  
352 photosynthetic capacity ( $P_N/C_c$  curves), light harvesting ( $P_N/PPFD$  curves) and  
353 diffusive limitations to CO<sub>2</sub> transport ( $G_{sH_2O}$ ,  $G_m$  and  $G_{totCO_2}$ ) of Siebold's beech  
354 indicated a high degree of overlap in the multi-variate space occupied by AA- and  
355 eO<sub>3</sub>-fumigated plants when measured in June (Fig. 5; student's t-test of PCA  
356 scores: component 1, P=0.215; component 2, P=0.646). However, the measurement  
357 month affected variations in component 1 and component 2, while O<sub>3</sub> was a  
358 significant factor affecting only component 1 (two-way ANOVA of PCA scores:  
359 component 1, O<sub>3</sub>: P<0.001, Month: P<0.001, O<sub>3</sub>×Month: P=0.002; component 2,  
360 O<sub>3</sub>: P=0.164, Month: P=0.029, O<sub>3</sub>×Month: P=0.059). In fact, eO<sub>3</sub>-treated plants did  
361 not overlap those treated by AA in August and October. In addition, Siebold's  
362 beech measured during October occupied distinct multivariate space in comparison  
363 to previous analyses in June and August. In this analysis, component 1 accounts  
364 for 49.2% of the variance within the dataset and component 2 accounts for 14.8%

365 of variance.

366

## 367 **Discussion**

### 368 **Ozone effects on mesophyll conductance and other photosynthetic parameters**

369 We analysed leaf gas exchange data in Siebold's beech exposed to elevated  $O_3$  to  
370 assess whether  $O_3$  affected  $G_m$ . We found that  $O_3$  caused a significant reduction of  
371  $G_m$  in August accompanied by a reduction of  $P_{N_{sat}}$  (Fig. 3B). On the other hand, no  
372 significant relationship between  $G_{sH_2O}$  and  $P_{N_{sat}}$  was found in  $eO_3$  (Fig. 3A). As a  
373 result,  $G_m$  could better explain the observed reduction of photosynthetic rate rather  
374 than  $G_{sH_2O}$  in  $eO_3$  (Table 3). In addition, the present study indicates that  $eO_3$  caused  
375 a decoupling of  $G_{sH_2O}$  from  $G_m$  (Fig. 3D), although a significant relationship has  
376 been previously found between  $G_{sH_2O}$  and  $G_m$  (Lloyd et al. 1992, Lauteri et al.  
377 2014). Although stomata generally regulate  $CO_2$  uptake, several studies have  
378 shown evidence that chronic  $O_3$  exposure impairs efficient stomatal control of gas  
379 exchange (Paoletti 2005, Hoshika et al. 2019, 2020).

380 In the previous report by Hoshika et al. (2013),  $O_3$  was found to decrease  $C_i$ -  
381 based  $V_{cmax}$  of Siebold's beech leaves in August and October based on the  
382 calculation from  $P_N/C_i$  curves assuming an infinite mesophyll conductance to  $CO_2$   
383 (Long and Bernacchi 2003). Such a decrease of  $C_i$ -based  $V_{cmax}$  is, however,  
384 attributed to a decreased  $G_m$  or degradation of Rubisco activity (Loreto et al. 1994).  
385 In the present study,  $O_3$  decreased  $G_m$  in August while  $C_c$ -based  $V_{cmax}$  was not  
386 significantly altered (Fig. 1E, Table 2), which is supported by previous findings in  
387 Siebold's beech (Watanabe et al. 2018a). In addition, we found that  $O_3$  exposure  
388 decreased  $C_c$ -based  $V_{cmax}$  and  $J_{max}$  in October while no reduction was found in  $G_{sH_2O}$ ,  
389  $G_m$  and  $G_{totCO_2}$ . The results suggest that a reduction in  $G_m$  may be a primary  
390 response in  $O_3$ -induced decrease of photosynthesis of Siebold's beech.

391

392 **Leaf age effects on mesophyll conductance and other photosynthetic**  
393 **parameters**

394 Mesophyll conductance ( $G_m$ ) decreased with leaf ageing, in association with a  
395 reduction of the leaf photosynthetic rate (Fig. 1A, E). Leaf morphological traits  
396 were not significantly correlated with  $G_m$  during the ageing process in control  
397 condition (AA). This is probably because the change in leaf morphology was small  
398 during leaf ageing in AA, although LD statistically significantly increased with  
399 season. Tosens et al. (2012) similarly reported the slow increase in LD and LMA  
400 with leaf ageing after leaf maturity in *Populus tremula*, while LT remained constant.  
401 The observed reduction of  $G_m$  in senescent leaves may be attributed to age-  
402 dependent alterations such as changes of chloroplasts number and size, the location  
403 of chloroplasts, photosynthetic enzyme content, and aquaporin status (Evans and  
404 Vellen 1996, Niinemets et al. 2009). In addition to  $G_m$ , most of photosynthetic  
405 parameters decreased with leaf ageing (Fig. 1, Table 2). Interestingly, the relative  
406 contribution to photosynthesis by mesophyll conductance ( $I_m$ ) was rather constant  
407 over the season (Table 3). Additionally, the stomatal limitation to photosynthesis  
408 ( $I_s$ ) decreased with leaf ageing, while the relative biochemical limitation ( $I_b$ )  
409 increased in the end of the growing season. It is known that stomata in senescent  
410 leaves remain open even in low light conditions, called the “dull leaf” phenomenon.  
411 They are, therefore, unable to regulate leaf gas exchange efficiently (Terashima,  
412 2002). On the other hand, the low biochemical photosynthetic capacity in senescent  
413 leaves was due to the decline of leaf nitrogen (Watanabe et al., 2018b), which may  
414 further limit photosynthesis in autumn. These results suggest that photosynthesis  
415 was primarily determined by diffusive limitations of CO<sub>2</sub> transport during summer  
416 in Siebold’s beech, while biochemical limitations were relatively important in

417 senescent leaves in autumn. This seasonal change is consistent with the PCA  
418 analysis for photosynthetic characteristics (Fig. 5).

419

#### 420 **Interactive effects of ozone and leaf age on leaf gas exchange**

421 Leaf senescence is often accelerated by O<sub>3</sub> exposure (Grulke and Heath 2020). The  
422 effects of O<sub>3</sub> on leaf gas exchange were similar to those of leaf senescence, i.e.  
423 significant reductions in the photosynthetic capacity, light harvesting and diffusive  
424 components of photosynthesis, but the reduction of photosynthetic capacity was  
425 observed earlier in eO<sub>3</sub> than in AA (Fig. 1A-F, Table 2). Mesophyll conductance  
426 ( $G_m$ ) showed a sharp decrease after O<sub>3</sub> exposure in August and no further change  
427 in October. Meanwhile, LD increased with leaf age especially at eO<sub>3</sub> (Table 1).  
428 Previous studies similarly reported that O<sub>3</sub> altered leaf cell ultrastructure in  
429 Siebold's beech (Yonekura et al. 2001) and increased LD in European beech  
430 (Bussotti et al. 2005). A larger LD may decrease CO<sub>2</sub> diffusion in the liquid phase  
431 and, thus,  $G_m$  (Niinemets 2015). As a result, a significant relationship between  $G_m$   
432 and LD over the season was found at eO<sub>3</sub> (Fig. 4C), suggesting that the reduction  
433 of  $G_m$  was accompanied by changes in the physical structure of mesophyll cells. It  
434 is known that some leaf structural changes are highlighted only when senescence  
435 is accelerated by environmental stress (Vollenweider et al. 2019). In fact, as a leaf  
436 age×O<sub>3</sub> interaction, inner cell wall thickening has been observed in aged leaves  
437 after O<sub>3</sub> exposure due to progressing cell injury in eO<sub>3</sub> (Günthardt-Goerg and  
438 Vollenweider 2007). However, we should note that the correlation between LD and  
439  $G_m$  was not strong ( $R^2 = 0.24$ ). This suggests that there may also be other factors  
440 causing a reduced  $G_m$  after O<sub>3</sub> exposure. For example, aquaporins are involved in  
441 the regulation of  $G_m$  (e.g. Hanba et al. 2004) and water across the bundle sheath  
442 (Shatil-Cohen et al. 2011). Ozone and the resultant reactive oxygen species (ROS)

443 reach the cell membrane (Vainonen and Kangasjärvi 2015), which may affect  $G_m$   
444 through direct effects on aquaporins. In fact,  $O_3$  may decrease leaf hydraulic  
445 conductance (Zhang et al. 2018), which is related to vein architecture in  
446 association with aquaporins (Scoffoni and Sack 2017). This hypothesis needs to be  
447 tested in further studies.

448 Limiting factors for the reduction of  $P_N$  after  $O_3$  exposure may vary with leaf  
449 age. In fact, diffusive resistances to  $CO_2$  transport were dominant factors for  
450 photosynthesis at  $eO_3$  in August, while the reduction of  $P_N$  after  $O_3$  exposure in  
451 October was mainly due to the co-limitation of  $V_{cmax}$  and  $J_{max}$  (Table 3). At the  
452 same time,  $O_3$  progressively increased the  $J_{max}/V_{cmax}$  ratio with leaf age (Table 2).  
453 This increase in  $J_{max}/V_{cmax}$  ratio suggests that the photosynthetic rate was limited  
454 more by Rubisco carbon fixation than RuBP regeneration by electron transport.  
455 Such a selective degradation of Rubisco quantity or activity was also observed in  
456 a poplar clone exposed to  $O_3$  (e.g. Bagard et al. 2008).

457 Rubisco activity is closely related to the capacity of photorespiration ( $R_{PR}$ )  
458 (Farquhar et al. 1980). In fact,  $R_{PR}$  in Siebold's beech was decreased by enhanced  
459  $O_3$  treatments with leaf ageing (Fig. 1C). The reduced  $R_{PR}$  is equivalent to reduced  
460 photoprotective function that, alongside a lower energy usage for photochemistry,  
461 would produce ROS, damaging photosynthetic biochemistry (Kangasjärvi et al.,  
462 2005). In addition, the plant photorespiratory system requires the glycine  
463 decarboxylase (GDC) reaction cycle in the mitochondria, which requires the  
464 oxidized form of nicotinamide adenine dinucleotide ( $NAD^+$ ) and generates NADH  
465 (the reduced form of NAD; Obata et al. 2016). This decrease in  $R_{PR}$  may result in  
466 a reduced  $NADH/NAD^+$  ratio stimulating mitochondrial respiration (Dizengremel  
467 et al. 2012) as confirmed here in the  $O_3$ -induced increase of dark respiration rate  
468 (Fig. 1B).

469

**470 Conclusion**

471 Our results indicate that O<sub>3</sub> damaged photosynthetic mechanisms in Siebold's  
472 beech leaves. Mesophyll conductance was associated with a reduced  
473 photosynthesis in O<sub>3</sub>-fumigated Siebold's beech in August. This O<sub>3</sub>-induced  
474 reduction of  $G_m$  was negatively correlated with leaf density, which was increased  
475 by O<sub>3</sub> exposure. This suggests that the reduction of  $G_m$  in August was accompanied  
476 by changes in the physical structure of mesophyll cells. However, the response of  
477 photosynthetic parameters to O<sub>3</sub> was different in the later growing season. In  
478 October, the O<sub>3</sub>-induced reduction of photosynthesis was mainly due to the co-  
479 limitation of  $V_{cmax}$  and  $J_{max}$  rather than diffusive resistances to CO<sub>2</sub> transport.  
480 Mesophyll conductance ( $G_m$ ) decreased in October due to leaf senescence  
481 regardless of O<sub>3</sub> treatments. In consequence, the O<sub>3</sub>-induced decrease of  $G_m$  was  
482 diminished. These results suggest that seasonal changes of the photosynthetic  
483 response to O<sub>3</sub> will be a key to modelling photosynthesis in an O<sub>3</sub>-polluted  
484 environment.

485

**486 Author contributions**

487 Y.H. conceived the study and methodology, and analysed leaf gas exchange data  
488 from the ozone FACE experiment performed by Y.H., M.W. and T.K.; M.H. co-  
489 conceived the study and contributed to the analysis of light-response curve. All  
490 authors were involved in writing the paper, although Y.H. took a lead role.

491

**492 Acknowledgement**

493 We are grateful to Mr. Naoki Inada and Mr. Tatsushiro Ueda for technical support.  
494 This work was partly supported by the Environment Research and Technology

495 Development Fund (B-1105) of the Ministry of the Environment, Japan, and by a  
496 Grant-in-aid from the Japanese Society for Promotion of Science (Type B  
497 23380078, Young Scientists B 24780239 and ditto B 15K16136) as well as JST,  
498 Japan (JPMJSC18HB) to MW and TK. We are also grateful for financial support to  
499 the LIFE+ project MOTTLES (LIFE15 ENV/IT/000183) of the European  
500 Commission.

501

#### 502 **Data availability statement**

503 Data sharing is not applicable to this article as all new created data is already  
504 contained within this article.

505

506

#### 507 **References**

- 508 Adachi S, Nakae T, Uchida M, Soda K, Takai T, Oi T, Yamamoto T, Ookawa T,  
509 Miyake H, Yano M, Hirasawa T (2013). The mesophyll anatomy enhancing CO<sub>2</sub>  
510 diffusion is a key trait for improving rice photosynthesis. *J Exp Bot* 64: 1061-  
511 1072
- 512 Bagard M, Jolivet Y, Hasenfratz-Sauder M-P, Gérard J, Dizengremel P, Le Thiec D  
513 (2015) Ozone exposure and flux-based response functions for photosynthetic  
514 traits in wheat, maize and poplar. *Environ Pollut* 206: 411–420
- 515 Bagard M, Le Thiec D, Delacote E, Hasenfratz-Sauder M-P, Banvoy J, Gérard J,  
516 Dizengremel P, Jolivet Y (2008) Ozone-induced changes in photosynthesis and  
517 photorespiration of hybrid poplar in relation to the developmental stage of the  
518 leaves. *Physiol Plant* 134: 559–574
- 519 Bussotti F, Agati G, Desotgiu R, Matteini P, Tani C (2005) Ozone foliar symptoms  
520 in woody plant species assessed with ultrastructural and fluorescence analysis.

- 521 New Phytol 166: 941–955
- 522 Dizengremel P, Vaultier M-N, Le Thiec D, Cabané M, Bagard M, Gérant D, Gérard  
523 J, Allah Dghim A, Richet N, Afif D, Pireaux J-C, Hasenfratz-Sauder M-P, Jolivet  
524 Y (2012) Phosphoenolpyruvate is at the crossroads of leaf metabolic responses  
525 to ozone stress. New Phytol 195: 512–517
- 526 Ethier GJ, Livingston NJ (2004) On the need to incorporate sensitivity to CO<sub>2</sub>  
527 transfer conductance into the Farquhar–von Caemmerer–Berry leaf  
528 photosynthesis model. Plant Cell Environ 27: 137–153
- 529 Evans JR, Vellen L (1996) Wheat cultivars differ in transpiration efficiency and  
530 CO<sub>2</sub> diffusion inside their leaves. In: Ishii R, Horie T (ed) Crop research in Asia:  
531 Achievements and perspective. Asian Crop Science Association, Tokyo, pp. 326–  
532 329
- 533 Fares S, Barta C, Brillì F, Centritto M, Ederli L, Ferranti F, Pasqualini S, Reale L,  
534 Tricoli D, Loreto F (2006) Impact of high ozone on isoprene emission,  
535 photosynthesis and histology of developing *Populus alba* leaves directly or  
536 indirectly exposed to the pollutant. Physiol Plant 128: 456–465
- 537 Farquhar GD, von Caemmerer S, Berry JA (1980) A biochemical model of  
538 photosynthetic CO<sub>2</sub> assimilation in leaves of C<sub>3</sub> species. Planta 149: 78–90
- 539 Fiscus EL, Booker FL, Burkey KO (2005) Crop responses to ozone: uptake, modes  
540 of action, carbon assimilation and partitioning. Plant Cell Environ 28: 997–1011
- 541 Flexas J, Díaz-Espejo A, Berry JA, Cifre J, Galmés J, Kaldenhoff R, Medrano H,  
542 Ribas-Carbó M (2007) Analysis of leakage in IRGA's leaf chambers of open gas  
543 exchange systems: quantification and its effects in photosynthesis  
544 parameterization. J Exp Bot 58: 1533–1543

- 545 Flowers MD, Fiscus EL, Burkey KO, Booker FL, Dubois JB (2007) Photosynthesis,  
546 chlorophyll fluorescence, and yield of snap bean (*Phaseolus vulgaris* L.)  
547 genotypes differing in sensitivity to ozone. *Environ Exp Bot*, 61: 190-198
- 548 Gago J, Carriquí M, Nadal M, Clemente-Moreno MJ, Coopman RE, Fernie AR,  
549 Flexas J (2019) Photosynthesis optimized across land plant phylogeny. *Trends*  
550 *Plant Sci* 24: 947-958
- 551 Galmes J, Flexas J, Keys AJ, Cifre J, Mitchell RAC, Madgwick PJ, Haslam RP,  
552 Medrano H, Parry MAJ (2005) Rubisco specificity factor tends to be larger in  
553 plant species from drier habitats and in species with persistent leaves. *Plant Cell*  
554 *Environ* 28: 571-579
- 555 Genty B, Briantais J-M, Baker NR (1989) The relationship between the quantum  
556 yield of photosynthetic electron transport and quenching of chlorophyll  
557 fluorescence. *Biochimica et Biophysica Acta (BBA)-General Subjects* 990: 87–  
558 92
- 559 Grantz DA, Shrestha A (2006) Tropospheric ozone and interspecific competition  
560 between Yellow nutsedge and Pima cotton. *Crop Sci* 46: 1879–1889
- 561 Grassi G, Magnani F (2005) Stomatal, mesophyll conductance and biochemical  
562 limitations to photosynthesis as affected by drought and leaf ontogeny in ash  
563 and oak trees. *Plant Cell Environ* 28: 834–849
- 564 Grulke NE, Heath RL (2020) Ozone effects on plants in natural ecosystems. *Plant*  
565 *Biol* 22 (S1): 12–37
- 566 Günthardt-Goerg MS, Matyssek R, Scheidegger C, Keller T (1993). Differentiation  
567 and structural decline in the leaves and bark of birch (*Betula pendula*) under low  
568 ozone concentrations. *Trees* 7: 104-114
- 569 Hanba YT, Shibasaka M, Hayashi Y, Hayakawa T, Kasamo K, Terashima I,  
570 Katsuhara M (2004). Overexpression of the barley aquaporin HvPIP2;1 increases

- 571 internal CO<sub>2</sub> conductance and CO<sub>2</sub> assimilation in the leaves of transgenic rice  
572 plants. *Plant Cell Physiol* 45: 521-529
- 573 Harley PC, Loreto, F., Dimarco, G., Sharkey, T.D. (1992) Theoretical  
574 considerations when estimating the mesophyll conductance to CO<sub>2</sub> flux by  
575 analysis of the response of photosynthesis to CO<sub>2</sub>. *Plant Physiol* 98: 1429-1436
- 576 Heath RL (1994). Possible mechanisms for the inhibition of photosynthesis by  
577 ozone. *Photosyn Res* 39: 439-451
- 578 Harley PC, Loreto, F., Dimarco, G., Sharkey, T.D. (1992) Theoretical  
579 considerations when estimating the mesophyll conductance to CO<sub>2</sub> flux by  
580 analysis of the response of photosynthesis to CO<sub>2</sub>. *Plant Physiol.*, **98**, 1429-1436
- 581 Hoshika Y, De Carlo A, Baraldi R, Neri L, Carrari E, Agathokleous E, Zhang L,  
582 Fares S, Paoletti E (2019) Ozone-induced impairment of night-time stomatal  
583 closure in O<sub>3</sub>-sensitive poplar clone is affected by nitrogen but not by  
584 phosphorus enrichment. *Sci Tot Environ* 692: 713-722
- 585 Hoshika Y, Fares S, Pellegrini E, Conte A, Paoletti E (2020) Water use strategy  
586 affects avoidance of ozone stress by stomatal closure in Mediterranean trees—  
587 A modelling analysis. *Plant Cell Environ* 43: 611-623
- 588 Hoshika Y, Watanabe M, Inada N, Koike T (2012) Modeling of stomatal ozone  
589 conductance for estimating ozone uptake of *Fagus crenata* under experimentally  
590 enhanced free-air ozone exposure. *Wat Air Soil Pollut* 223: 3893-3901
- 591 Hoshika Y, Watanabe M, Inada N, Koike T (2013) Model-based analysis of  
592 avoidance of ozone stress by stomatal closure in Siebold's beech (*Fagus*  
593 *crenata*). *Ann Bot* 112: 1149-1158
- 594 Ivanova LA, Yudina PK, Ronzhina DA, Ivanov LA, Hölzel N (2018) Quantitative  
595 mesophyll parameters rather than whole-leaf traits predict response of C<sub>3</sub> steppe  
596 plants to aridity. *New Phytol* 217: 558-570

- 597 Izuta T (2017) Air Pollution Impacts on Plants in East Asia. Springer-Verlag, Tokyo
- 598 Kaipiainen EL (2009) Parameters of photosynthesis light curve in *Salix dasyclados*  
599 and their changes during the growth season. Russian J Plant Physiol 56: 445-453
- 600 Kangasjärvi J, Jaspers P, Kollist H (2005) Signalling and cell death in ozone-  
601 exposed plants. Plant Cell Environ 28: 1021-1036
- 602 Killi D, Haworth M (2017) Diffusive and metabolic constraints to photosynthesis  
603 in Quinoa during drought and salt stress. Plants 6: 49
- 604 Kirschbaum MU, Farquhar GD (1987) Investigation of the CO<sub>2</sub> dependence of  
605 quantum yield and respiration in *Eucalyptus pauciflora*. Plant Physiol 83: 1032-  
606 1036
- 607 Koike T, Kato S, Shimamoto Y, Kitamura K, Kawano S, Ueda K, Mikami T (1998)  
608 Mitochondrial DNA variation follows a geographic pattern in Japanese beech  
609 species. Botanica Acta 111: 87-92
- 610 Kok B (1948) A critical consideration of the quantum yield of Chlorella  
611 photosynthesis. Enzymologia 13: 1-56
- 612 Laisk A, Loreto F (1996) Determining photosynthetic parameters from leaf CO<sub>2</sub>  
613 exchange and chlorophyll fluorescence: Rubisco specificity factor, dark  
614 respiration in the light, excitation distribution between photosystems,  
615 alternative electron transport rate and mesophyll diffusion resistance. Plant  
616 Physiol 110: 903-912
- 617 Lauteri M, Haworth M, Serraj R, Monteverdi MC, Centritto M (2014)  
618 Photosynthetic diffusional constraints affect yield in drought stressed rice  
619 cultivars during flowering. Plos one 9: e109054
- 620 Long SP, Bernacchi CJ (2003) Gas exchange measurements, what can they tell us  
621 about the underlying limitations to photosynthesis? Procedures and sources of  
622 error. J Exp Bot 54: 2393-2401

- 623 Loreto F, Di Marco G, Tricoli D, Sharkey TD (1994) Measurements of mesophyll  
624 conductance, photosynthetic electron transport and alternative electron sinks of  
625 field grown wheat leaves. *Photosyn Res* 41: 397–403
- 626 Loreto F, Harley PC, Di Marco G, Sharkey TD (1992) Estimation of mesophyll  
627 conductance to CO<sub>2</sub> flux by three different methods. *Plant Physiol* 98: 1437–  
628 1443
- 629 Marino G, Haworth M, Scartazza A, Tognetti R, Centritto M (2020) A Comparison  
630 of the variable J and carbon-isotopic composition of sugars methods to assess  
631 mesophyll conductance from the leaf to the canopy scale in drought-stressed  
632 cherry. *Int J Mol Sci* 21(4): 1222
- 633 Matyssek R, Schnyder H, Oßwald W, Ernst D, Munch JC, Pretzsch H (2012) Growth  
634 and Defence in Plants; Resource Allocation at Multiple Scales. Springer V.,  
635 Heidelberg, 470 pp
- 636 Matyssek R, Clarke N, Cudlin P, Mikkelsen TN, Tuovinen JP, Wieser G, Paoletti E  
637 (2013) Climate change, air pollution and global challenges: understanding and  
638 perspectives from forest research. *Developments in Environmental Science* 13.  
639 Elsevier, Amsterdam, 622 pp
- 640 Mills G, Pleijel H, Malley CS, Sinha B, Cooper O, Schultz M, Neufeld HS, Simpson  
641 D, Sharps K, Feng Z, Gerosa G, Harmens H, Kobayashi K, Saxena P, Paoletti E,  
642 Sinha V, Xu X (2018) Tropospheric Ozone Assessment Report: Present day  
643 tropospheric ozone distribution and trends relevant to vegetation. *Elementa*  
644 *Science of the Anthropocene* 6(1): 47
- 645 Moura BB, Alves ES, Marabesi MA, de Souza SR, Schaub M, Vollenweider P  
646 (2018). Ozone affects leaf physiology and causes injury to foliage of native tree  
647 species from the tropical Atlantic Forest of southern Brazil. *Sci Tot Environ* 610-  
648 611: 912-925

- 649 Niinemets Ü (2015) Is there a species spectrum within the world-wide leaf  
650 economics spectrum? Major variations in leaf functional traits in the  
651 Mediterranean sclerophyll *Quercus ilex*. *New Phytol* 205: 79–96
- 652 Niinemets Ü, Díaz-Espejo A, Flexas J, Galmés J, Warren CR (2009) Role of  
653 mesophyll diffusion conductance in constraining potential photosynthetic  
654 productivity in the field. *J Exp Bot* 60: 2249–2270
- 655 Obata T, Florian A, Timm S, Bauwe H, Fernie AR (2016). On the metabolic  
656 interactions of (photo)respiration. *J Exp Bot* 67: 3003–3014
- 657 Oksanen E (2005). Northern conditions enhance the susceptibility of birch (*Betula*  
658 *pendula* Roth) to oxidative stress caused by ozone. In: Omasa K, Nouchi I, De  
659 Kok LJ (ed) *Plant responses to air pollution and global change*. Springer-Verlag,  
660 Tokyo, pp 29–35
- 661 Onoda Y, Wright IJ, Evans JR, Hikosaka K, Kitajima K, Niinemets Ü, Poorter H,  
662 Tosens T, Westoby M (2017) Physiological and structural tradeoffs underlying  
663 the leaf economics spectrum. *New Phytol* 214: 1447–1463
- 664 Paoletti E (2005) Ozone slows stomatal response to light and leaf wounding in a  
665 Mediterranean evergreen broadleaf, *Arbutus unedo*. *Environ Pollut* 134: 439–  
666 445
- 667 Pääkkönen E, Holopainen T, Kärenlampi L (1995). Ageing-related anatomical and  
668 ultrastructural changes in leaves of birch (*Betula pendula* Roth.) clones as  
669 affected by low ozone exposure. *Ann Bot* 75: 285–294
- 670 Poorter H, Niinemets Ü, Poorter I, Wright IJ, Villar R (2009). Causes and  
671 consequences of variation in leaf mass per area (LMA): a meta-analysis. *New*  
672 *Phytol* 182: 565–588
- 673 R Core Team (2018) *R: A language and environment for statistical computing*.  
674 Vienna, Austria: R Foundation for Statistical Computing. Retrieved from

- 675 <https://www.R-project.org/>
- 676 Scoffoni C, Sack L (2017) The causes and consequences of leaf hydraulic decline  
677 with dehydration. *J Exp Bot* 68: 4479-4496
- 678 Sharkey TD (1988) Estimating the rate of photorespiration in leaves. *Physiol Plant*  
679 73: 147– 152
- 680 Shatil-Cohen A, Attia Z, Moshelion M (2011). Bundle-sheath cell regulation of  
681 xylem-mesophyll water transport via aquaporins under drought stress: a target  
682 of xylem-borne ABA? *The Plant J* 67: 72-80
- 683 Terashima I. (2002) Photosynthesis at leaf and individual level. In: Sato K (ed)  
684 Photosynthesis. Asakura, Tokyo, pp. 125-149 (in Japanese)
- 685 Terashima I, Ishibashi M, Ono K, Hikosaka K (1995). Three resistances to CO<sub>2</sub>  
686 diffusion: leaf-surface water, intercellular spaces and mesophyll cells. In:  
687 Mathis P (ed) Photosynthesis: from light to biosphere, Vol. V. Kluwer Academic  
688 Publishers, Dordrecht, pp. 537–542
- 689 Tomás M, Flexas J, Copolovici L, Galmés J, Hallik L, Medrano H, Ribas-Carbó M,  
690 Tosens T, Vislap V, Niinemets Ü (2013). Importance of leaf anatomy in  
691 determining mesophyll diffusion conductance to CO<sub>2</sub> across species:  
692 quantitative limitations and scaling up by models. *J Exp Bot* 64: 2269-2281
- 693 Tosens T, Niinemets Ü, Vislap V, Eichelmann H, Diez PC (2012) Developmental  
694 changes in mesophyll diffusion conductance and photosynthetic capacity under  
695 different light and water availabilities in *Populus tremula*: how structure  
696 constrains function. *Plant Cell Environ* 35: 839–856
- 697 Vainonen JP, Kangasjärvi J (2015) Plant signaling in acute ozone exposure. *Plant*  
698 *Cell Environ* 38: 240-252
- 699 Velikova V, Tsonev T, Pinelli P, Alessio GA, Loreto F (2005) Localized ozone  
700 fumigation system for studying ozone effects on photosynthesis, respiration,

- 701 electron transport rate and isoprene emission in field-grown Mediterranean oak  
702 species. *Tree Physiol* 25: 1523-1532
- 703 Veromann-Jürgenson L-L, Brodribb TJ, Niinemets Ü, Tosens T (2020) Pivotal role  
704 of mesophyll conductance in shaping photosynthetic performance across 67  
705 structurally diverse gymnosperm species. *Int J Plant Sci* 181: 116-128
- 706 Watanabe M, Hoshika Y, Inada N, Koike T (2014a) Canopy carbon budget of  
707 Siebold's beech (*Fagus crenata*) sapling under free air ozone exposure. *Environ*  
708 *Pollut* 184: 682-689
- 709 Watanabe M, Hoshika Y, Inada N, Koike T (2018b) Photosynthetic activity in  
710 relation to a gradient of leaf nitrogen content within a canopy of Siebold's beech  
711 and Japanese oak saplings under elevated ozone. *Sci Tot Environ* 636: 1455-  
712 1462
- 713 Watanabe M, Hoshika Y, Inada N, Wang X, Mao Q, Koike T (2013) Photosynthetic  
714 traits of Siebold's beech and oak saplings grown under free air ozone exposure.  
715 *Environ Pollut* 174: 50-56
- 716 Watanabe M, Hoshika Y, Koike T (2014b) Photosynthetic responses of Monarch  
717 birch seedlings to differing timings of free air ozone fumigation. *J Plant Res*  
718 127: 339-345
- 719 Watanabe M, Komimaki Y, Mori M, Okabe S, Arakawa I, Kinose Y, Izuta T (2018a)  
720 Mesophyll conductance to CO<sub>2</sub> in leaves of Siebold's beech (*Fagus crenata*)  
721 seedlings under elevated ozone. *J Plant Res* 131: 907-914
- 722 Watanabe M, Yamaguchi M, Matsumura H, Kohno Y, Izuta T (2012) Risk  
723 assessment of ozone impact on *Fagus crenata* in Japan: consideration of  
724 atmospheric nitrogen deposition. *Europ J For Res* 131: 475-484

- 725 Warren CR, Löw M, Matyssek R, Tausz M (2007) Internal conductance to CO<sub>2</sub>  
726 transfer of adult *Fagus sylvatica*: Variation between sun and shade leaves and  
727 due to free-air ozone fumigation. *Environ Exp Bot* 59: 130-138
- 728 Xu Y, Feng Z, Shang B, Dai L, Uddling J, Tarvainen L (2019) Mesophyll  
729 conductance limitation of photosynthesis in poplar under elevated ozone. *Sci Tot*  
730 *Environ* 657: 136-145
- 731 Yamaguchi M, Watanabe M, Matsumura H, Kohno Y, Izuta T (2011) Experimental  
732 studies on the effects of ozone on growth and photosynthetic activity of Japanese  
733 forest tree species. *Asian J Atmos Environ* 5: 65-78, doi:  
734 10.5572/ajae.2011.5.2.065
- 735 Yonekura T, Honda Y, Oksanen E, Yoshidome M, Watanabe M, Funada R, Koike T,  
736 Izuta T (2001) The influences of ozone and soil water stress, singly and in  
737 combination, on leaf gas exchange rates, leaf ultrastructural characteristics and  
738 annual ring width of *Fagus crenata* seedlings. *J Jpn Soc Atmos Environ* 36: 333-  
739 351
- 740 Zhang WW, Wang M, Wang AY, Yin XH, Feng ZZ, Hao GY (2018) Elevated ozone  
741 concentration decreases whole-plant hydraulic conductance and disturbs water  
742 use regulation in soybean plants. *Physiol Plant* 163: 183-195

743

#### 744 **Supporting information**

745 Additional Supporting Information may be found in the online version of this  
746 article:

747 **Fig. S1.** Responses of net photosynthetic rate ( $P_N$ ) to the sub-stomatal  
748 concentration of CO<sub>2</sub> ( $C_i$ ) or the concentration of CO<sub>2</sub> inside the chloroplast  
749 envelope ( $C_c$ ).

750 **Fig. S2.** Relationship between mesophyll conductance ( $G_m$ ) values derived from  
751 the variable J method and those derived from the  $P_N/C_i$  curve fitting method.

752 **Fig. S3.** Relationships between leaf gas exchange parameters and leaf mass per

753 area (LMA) of Siebold's beech saplings.

754 **Fig. S4.** Relationships between leaf gas exchange parameters and leaf thickness  
755 (LT) of Siebold's beech saplings.

756

757

#### 758 **Figure legends**

759 **Figure 1.** Photosynthetic parameters of Siebold's beech grown under ambient (AA)  
760 and elevated O<sub>3</sub> (eO<sub>3</sub>). (A) Light-saturated net photosynthetic rate [ $P_{N_{sat}}$ ], (B) dark  
761 respiration rate [ $R_N$ ], (C) photorespiration [ $R_{PR}$ ], (D) stomatal conductance to water  
762 vapor [ $G_{sH_2O}$ ], (E) mesophyll conductance to CO<sub>2</sub> [ $G_m$ ], (F) total conductance to  
763 CO<sub>2</sub> [ $G_{totCO_2}$ ]. Each value is the mean  $\pm$  standard error (n=6). Two-way ANOVA: \*  
764  $P < 0.05$ , \*\*  $P < 0.01$ , \*\*\*  $P < 0.001$ , ns denotes not significant. Different letters show  
765 significant differences among treatments ( $P < 0.05$ , Tukey test).

766 **Figure 2.** Responses of net photosynthetic rate ( $P_N$ ), stomatal conductance ( $G_{sH_2O}$ ),  
767 mesophyll conductance ( $G_m$ ) and electron transport rate (ETR) to photosynthetic  
768 photon flux density (PPFD). The  $P_N$ /PPFD curves were obtained by measuring  $P_N$   
769 over 11 PPFD steps (1500, 1100, 800, 500, 400, 300, 200, 100, 75, 50, 0  $\mu\text{mol m}^{-2}$   
770  $\text{s}^{-1}$ ) in Siebold's beech exposed to different O<sub>3</sub> concentrations (ambient [AA] or  
771 elevated O<sub>3</sub> [eO<sub>3</sub>]). Each value is the mean  $\pm$  standard error (n=6).

772 **Figure 3.** Relationships between (A) light-saturated net photosynthetic rate [ $P_{N_{sat}}$ ]  
773 and stomatal conductance for water vapor [ $G_{sH_2O}$ ], (B)  $P_N$  and mesophyll  
774 conductance to CO<sub>2</sub> [ $G_m$ ], (C)  $P_N$  and total conductance to CO<sub>2</sub> [ $G_{totCO_2}$ ], (D)  $G_m$   
775 and  $G_{sH_2O}$ , in Siebold's beech. Linear regression analysis was used to assess the  
776 significance of the relationship in ambient (AA) and elevated O<sub>3</sub> (eO<sub>3</sub>). \*  $P < 0.05$ ,  
777 \*\*\*  $P < 0.001$ , ns denotes not significant.

778 **Figure 4.** Relationships between leaf gas exchange parameters (light-saturated net  
779 photosynthetic rate [ $P_{N_{sat}}$ ], stomatal conductance [ $G_{sH_2O}$ ], mesophyll conductance

780 [ $G_m$ ] and total conductance to  $\text{CO}_2$  [ $G_{\text{totCO}_2}$ ] and leaf density (LD) of Siebold's  
781 beech saplings under different  $\text{O}_3$  concentrations (ambient [AA] or elevated  $\text{O}_3$   
782 [ $e\text{O}_3$ ]). Simple linear regression analysis was applied to assess the relationships. \*  
783  $P < 0.05$ , ns denotes not significant.

784 **Figure 5.** Principal component analysis of parameters derived from analyses of the  
785 photosynthetic capacity ( $P_N/C_c$  curves), light harvesting ( $P_N/\text{PPFD}$  curves) and  
786 diffusive limitations to  $\text{CO}_2$  transport ( $G_{s\text{CO}_2}$ ,  $G_m$  and  $G_{\text{totCO}_2}$ ) of Siebold's beech  
787 grown under different  $\text{O}_3$  concentrations (ambient [AA] or elevated  $\text{O}_3$  [ $e\text{O}_3$ ]).  
788 Ellipses represent 95% confidence intervals for measurements conducted in June,  
789 August and October. The correlation circle is also shown. Measurements of AA-  
790 treated plants in June and August and  $e\text{O}_3$ -treated plants in June occupy the same  
791 position in multi-variate space. On the other hand,  $e\text{O}_3$ -treated plants analysed in  
792 October occupy statistically distinct multi-variate space. Component 1 accounts  
793 for 49.2% of the variance within the dataset and component 2 accounts for 14.8%  
794 of variance.

795

796

797

798

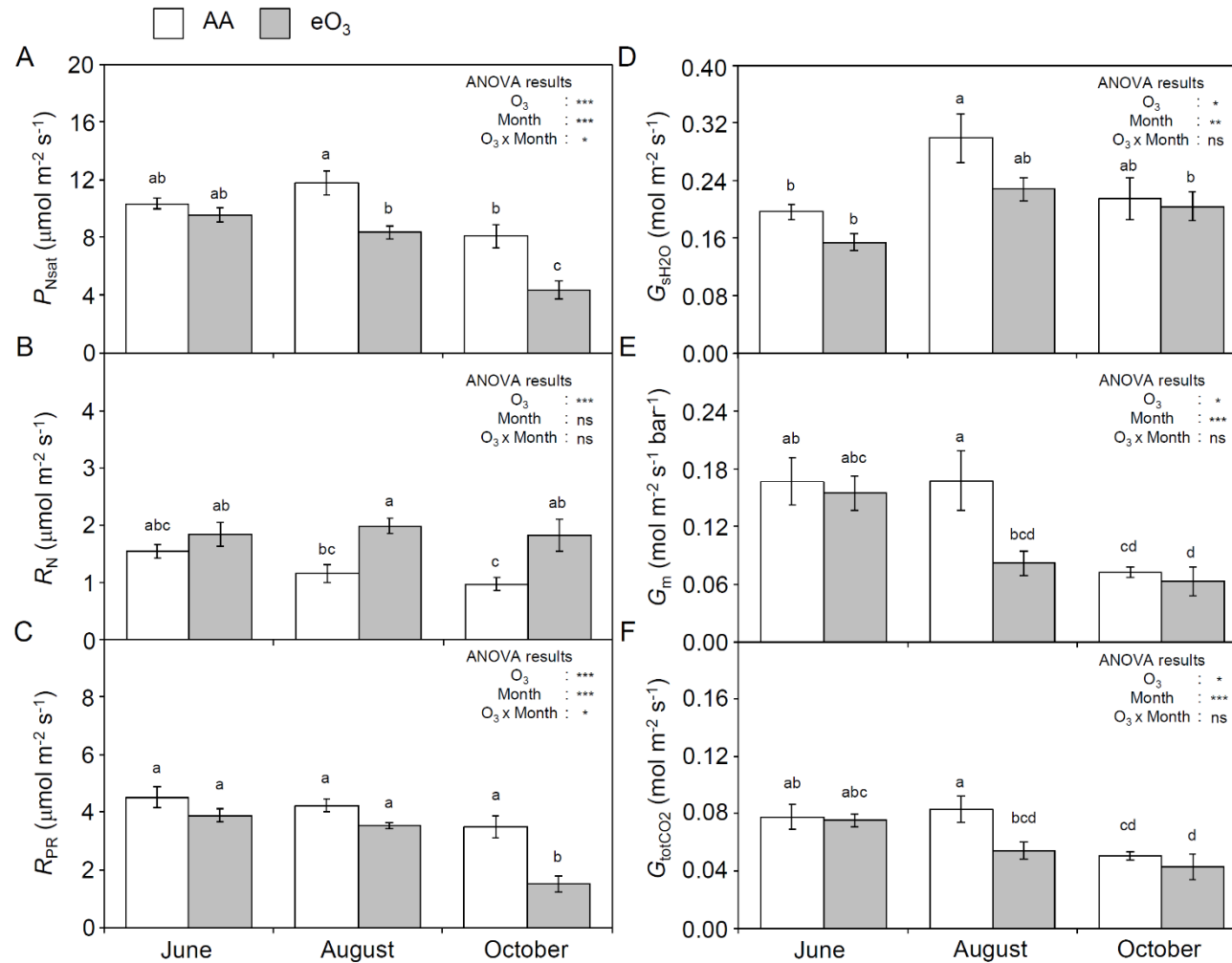


**Figure 1.** Photosynthetic parameters of Siebold's beech grown under ambient (AA) and elevated O<sub>3</sub> (eO<sub>3</sub>): (A) Light-saturated net photosynthetic rate [ $P_{N_{sat}}$ ], (B) dark respiration rate [ $R_N$ ], (C) photorespiration [ $R_{PR}$ ], (D) stomatal conductance to water vapor [ $G_{sH_2O}$ ], (E) mesophyll conductance to CO<sub>2</sub> [ $G_m$ ], (F) total conductance to CO<sub>2</sub> [ $G_{totCO_2}$ ]. Each value is the mean  $\pm$  standard error (n = 6). Two-way ANOVA: \*  $p < 0.05$ , \*\*  $p < 0.01$ , \*\*\*  $p < 0.001$ , ns denotes not significant. Different letters show significant differences among treatments ( $p < 0.05$ , Tukey test).



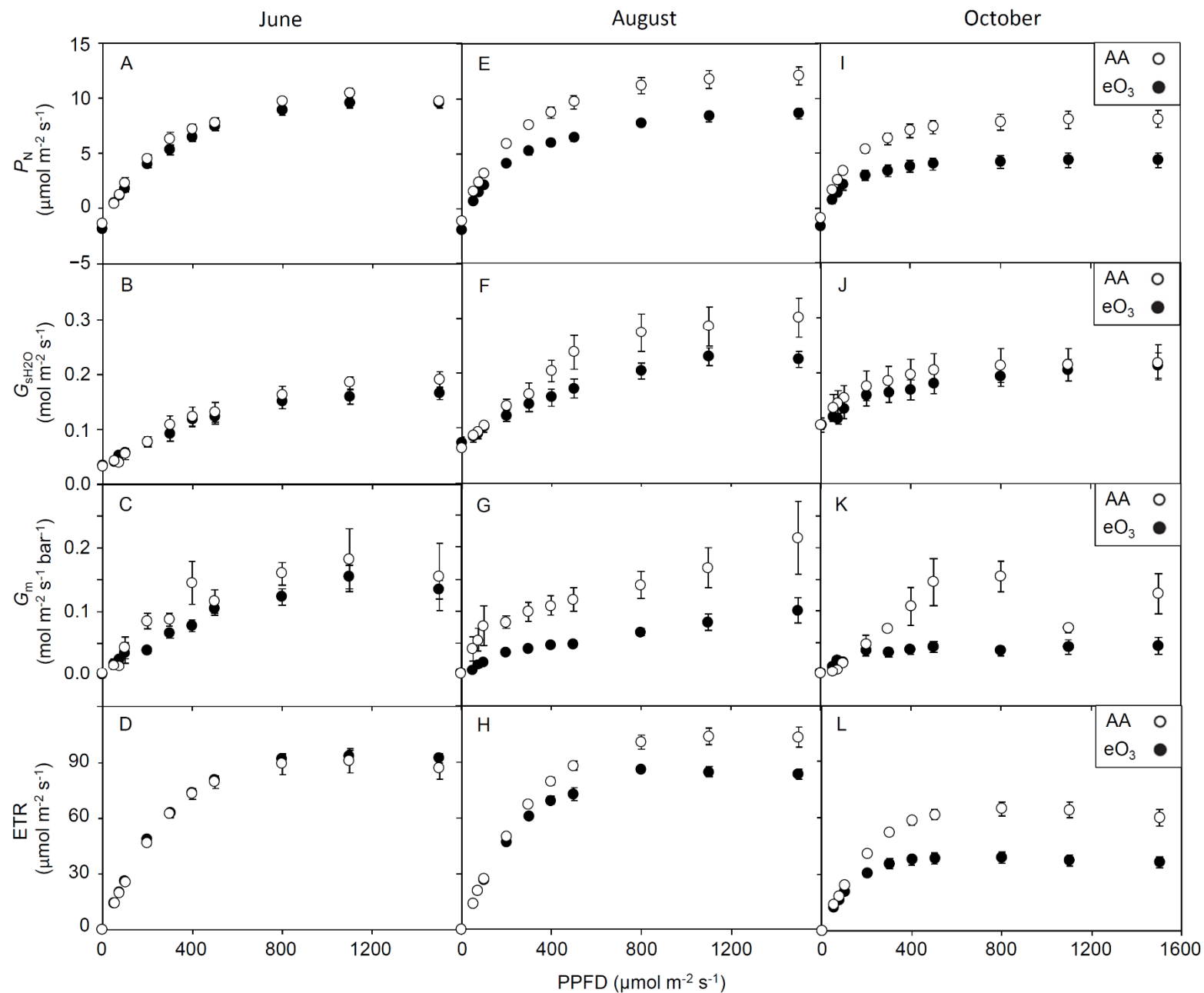


**Figure 2.** Responses of net photosynthetic rate ( $P_N$ ), stomatal conductance ( $G_{SH_2O}$ ), mesophyll conductance ( $G_m$ ) and electron transport rate (ETR) to

photosynthetic photon flux density (PPFD). The  $P_N$ /PPFD curves were obtained by measuring  $P_N$  over 11 PPFD steps (1500, 1100, 800, 500, 400, 300, 200, 100, 75, 50, 0  $\mu\text{mol m}^{-2} \text{s}^{-1}$ ) in Siebold's beech exposed to different  $\text{O}_3$  concentrations (ambient [AA] or elevated  $\text{O}_3$  [e $\text{O}_3$ ]). Each value is the mean  $\pm$  standard error (n = 6).

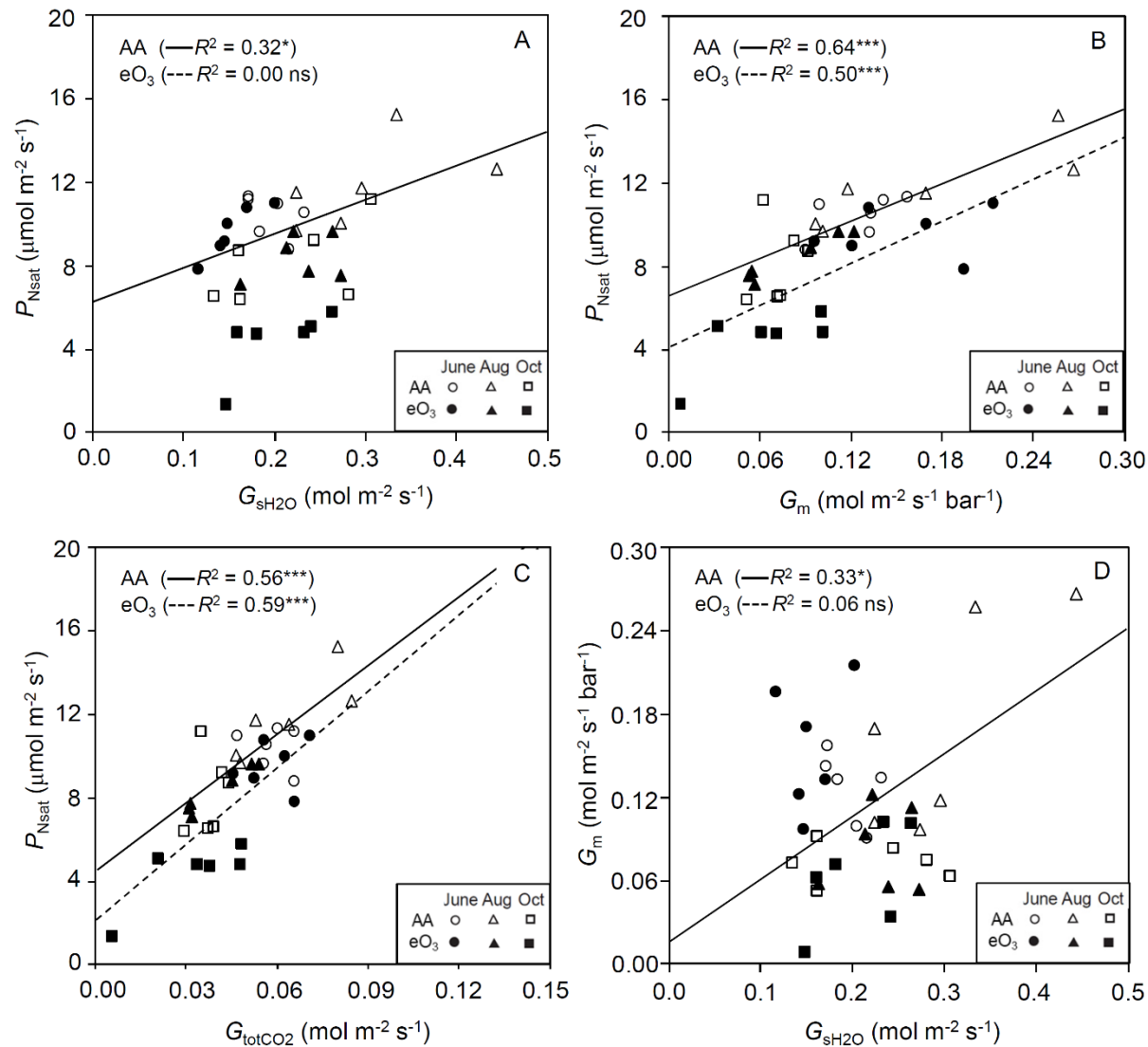


**Figure 3.** Relationships between (A) light-saturated net photosynthetic rate [ $P_{Nsat}$ ] and stomatal conductance for water vapor [ $G_{sH_2O}$ ], (B)  $P_N$  and mesophyll conductance to CO<sub>2</sub> [ $G_m$ ], (C)  $P_N$  and total conductance to CO<sub>2</sub> [ $G_{totCO_2}$ ], (D)  $G_m$  and  $G_{sH_2O}$ , in Siebold's beech. Linear regression analysis was used to assess

the significance of the relationship in ambient (AA) and elevated O<sub>3</sub> (eO<sub>3</sub>). \*  $p < 0.05$ , \*\*\*  $p < 0.001$ , ns denotes not significant.

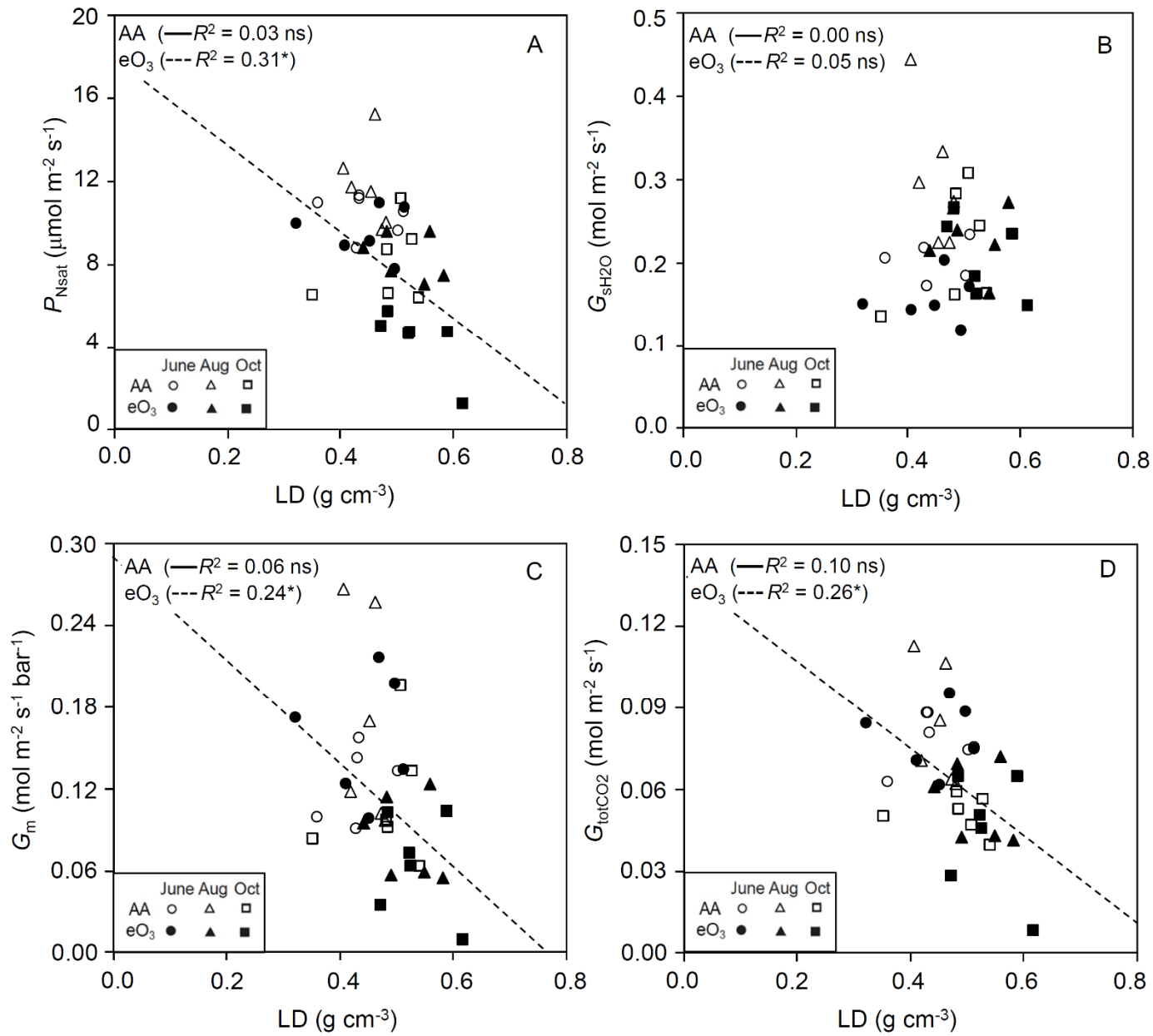


**Figure 4.** Relationships between leaf gas exchange parameters (A: light-saturated net photosynthetic rate [ $P_{\text{Nsat}}$ ], B: stomatal conductance [ $G_{\text{SH}_2\text{O}}$ ], C: mesophyll

conductance [ $G_m$ ] and D: total conductance to  $CO_2$  [ $G_{totCO_2}$ ] and leaf density (LD) of Siebold's beech saplings under different  $O_3$  concentrations (ambient [AA] or elevated  $O_3$  [ $eO_3$ ]). Simple linear regression analysis was applied to assess the relationships. \*  $p < 0.05$ , ns denotes not significant.

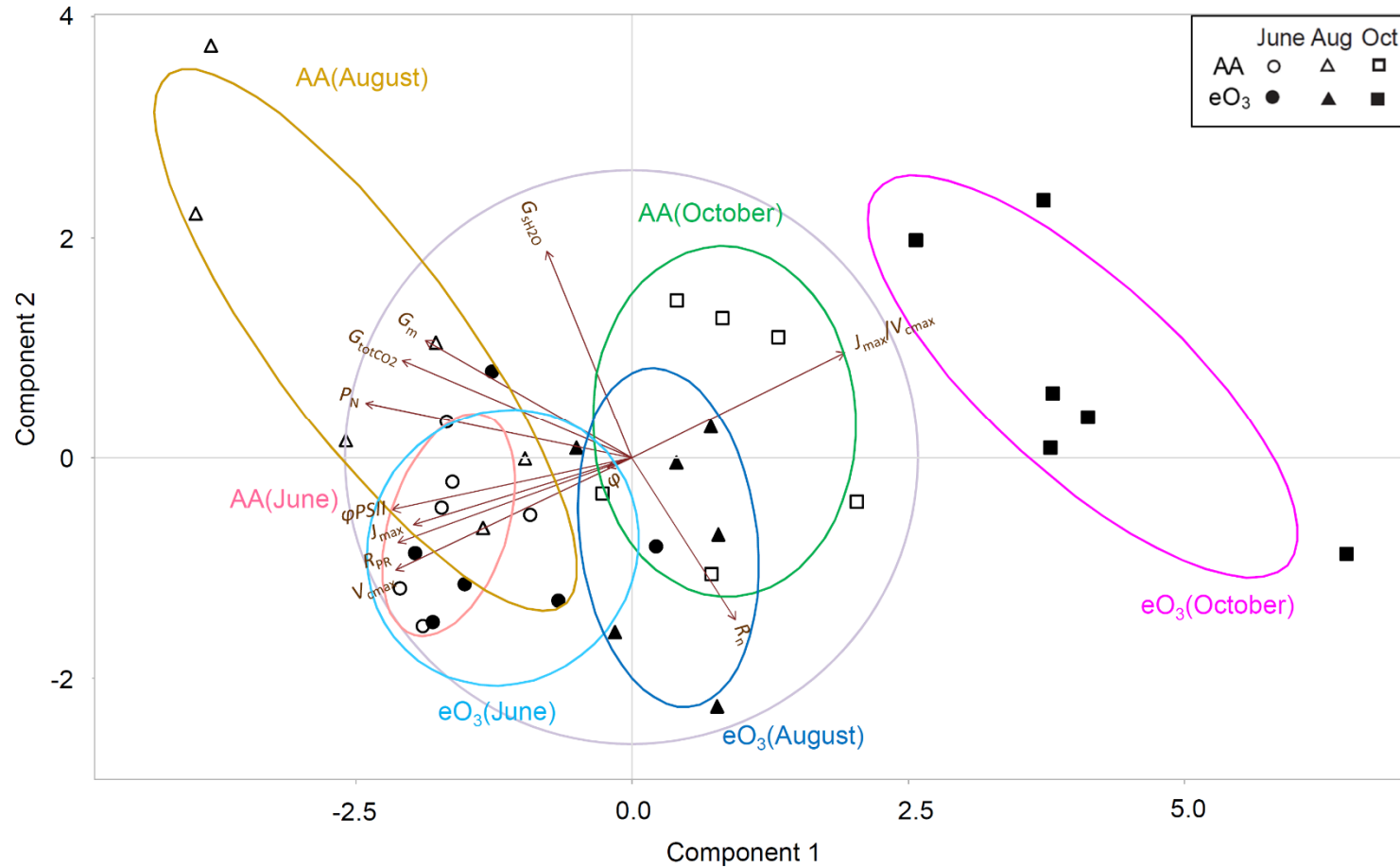


**Figure 5.** Principal component analysis of parameters derived from analyses of the photosynthetic capacity ( $P_N/C_c$  curves), light harvesting ( $P_N/PPFD$  curves) and diffusive limitations to CO<sub>2</sub> transport ( $G_{sCO_2}$ ,  $G_m$  and  $G_{totCO_2}$ ) of Siebold's beech grown under different O<sub>3</sub> concentrations (ambient [AA] or elevated O<sub>3</sub> [eO<sub>3</sub>]). Ellipses represent 95% confidence intervals for measurements conducted in June, August and October. The correlation circle is also shown. Measurements of AA-treated plants in June and August and eO<sub>3</sub>-treated plants in June occupy the same position in multi-variate space. On the other hand, eO<sub>3</sub>-treated plants analysed in October occupy statistically distinct multi-variate space. Component 1 accounts for 49.2% of the variance within the dataset and

component 2 accounts for 14.8% of variance.

**Table 1** Leaf mass per area (LMA), leaf density (LD) and leaf thickness (LT) of Siebold's beech saplings grown under ambient (AA) and elevated O<sub>3</sub> (eO<sub>3</sub>) measured in 2012. Each value is the mean ± standard error (n = 6). Two-way ANOVA: \*  $p < 0.05$ , ns denotes not significant. Different letters show significant differences among treatments ( $p < 0.05$ , Tukey test).

	LMA (g m <sup>-2</sup> )				LD (g cm <sup>-3</sup> )				LT (mm)			
	AA		eO <sub>3</sub>		AA		eO <sub>3</sub>		AA		eO <sub>3</sub>	
June	90.9 ± 7.3	a	83.0 ± 6.0	a	0.45 ± 0.02	ab	0.44 ± 0.03	a	0.20 ± 0.01	a	0.19 ± 0.01	a
August	81.3 ± 3.0	a	92.0 ± 2.6	a	0.45 ± 0.01	ab	0.52 ± 0.02	bc	0.18 ± 0.01	a	0.18 ± 0.00	a
October	90.8 ± 8.0	a	96.6 ± 4.4	a	0.48 ± 0.03	abc	0.54 ± 0.02	c	0.19 ± 0.01	a	0.18 ± 0.00	a
<i>ANOVA results</i>												
O <sub>3</sub>		ns				*				ns		
Month		ns				*				ns		
O <sub>3</sub> × Month		ns				ns				ns		

**Table 2** Parameters derived from analyses of light harvesting ( $P_N$ /PPFD curves: initial slope of photosynthetic light response curve [ $\Phi$ ], quantum yield of photosystem II photochemistry [ $\phi$ PSII], electron transport rate [ETR]) and photosynthetic capacity ( $P_N$ /Cc curve: maximum rate of carboxylation [ $V_{\text{cmax}}$ ], maximum rate of electron transport for RuBP regeneration [ $J_{\text{max}}$ ], the ratio of  $J_{\text{max}}$  to  $V_{\text{cmax}}$  [ $J_{\text{max}}/V_{\text{cmax}}$  ratio]) of Siebold's beech grown under ambient (AA) and elevated  $\text{O}_3$  (e $\text{O}_3$ ). Each value is the mean  $\pm$  standard error (n = 6). Two-way ANOVA: \*  $p < 0.05$ , \*\*  $p < 0.01$ , \*\*\*  $p < 0.001$ , ns denotes not significant. Different letters show significant differences among treatments ( $p < 0.05$ , Tukey test).

	$\Phi$ (mol mol <sup>-1</sup> )				$\phi$ PSII				ETR ( $\mu\text{mol m}^{-2} \text{s}^{-1}$ )			
	AA		e $\text{O}_3$		AA		e $\text{O}_3$		AA		e $\text{O}_3$	
June	0.042 $\pm$ 0.003	a	0.037 $\pm$ 0.002	a	0.20 $\pm$ 0.01	ab	0.20 $\pm$ 0.01	ab	91.0 $\pm$ 6.0	ab	93.4 $\pm$ 3.2	ab
August	0.043 $\pm$ 0.002	a	0.041 $\pm$ 0.001	a	0.22 $\pm$ 0.01	a	0.18 $\pm$ 0.01	b	103.8 $\pm$ 4.6	a	84.8 $\pm$ 2.7	b
October	0.044 $\pm$ 0.001	a	0.038 $\pm$ 0.004	a	0.14 $\pm$ 0.01	c	0.08 $\pm$ 0.01	d	64.3 $\pm$ 4.0	c	37.6 $\pm$ 2.9	d
<b>ANOVA results</b>												
$\text{O}_3$		ns				***				***		
Month		ns				***				***		
$\text{O}_3 \times \text{Month}$		ns				**				**		

	$V_{\text{cmax}}$ ( $\mu\text{mol m}^{-2} \text{s}^{-1}$ )				$J_{\text{max}}$ ( $\mu\text{mol m}^{-2} \text{s}^{-1}$ )				$J_{\text{max}}/V_{\text{cmax}}$ ratio			
	AA		e $\text{O}_3$		AA		e $\text{O}_3$		AA		e $\text{O}_3$	
June	66.8 $\pm$ 6.9	a	62.7 $\pm$ 6.1	a	118.0 $\pm$ 7.8	ab	114.9 $\pm$ 10.1	ab	1.8 $\pm$ 0.1	a	1.9 $\pm$ 0.1	a
August	63.2 $\pm$ 2.5	a	54.5 $\pm$ 6.0	a	113.5 $\pm$ 1.8	ab	87.9 $\pm$ 6.4	bc	1.8 $\pm$ 0.1	a	1.7 $\pm$ 0.2	a
October	47.2 $\pm$ 4.9	a	24.8 $\pm$ 2.4	b	95.2 $\pm$ 3.4	abc	70.1 $\pm$ 6.1	c	2.1 $\pm$ 0.2	a	2.9 $\pm$ 0.1	b
<b>ANOVA results</b>												
$\text{O}_3$		**				**				*		
Month		***				***				***		
$\text{O}_3 \times \text{Month}$		ns				ns				**		

**Table 3** Relative contribution of stomatal, mesophyll conductance and biochemical limitations ( $l_s$ ,  $l_m$  and  $l_b$ , respectively) to light-saturated net photosynthesis ( $P_{N_{sat}}$ ) of Siebold's beech grown under ambient (AA) and elevated  $O_3$  (e $O_3$ ). Each value is the mean  $\pm$  standard error (n = 6). Two-way ANOVA: \*  $p < 0.05$ , \*\*  $p < 0.01$ , \*\*\*  $p < 0.001$ , ns denotes not significant. Different letters show significant differences among treatments ( $p < 0.05$ , Tukey test).

	$l_s$ (%)		$l_m$ (%)		$l_b$ (%)							
	AA	e $O_3$	AA	e $O_3$	AA	e $O_3$						
June	27.9 $\pm$ 0.8	ab	35.1 $\pm$ 2.1	a	35.2 $\pm$ 4.7	a	29.6 $\pm$ 4.4	a	36.9 $\pm$ 5.1	ab	35.3 $\pm$ 2.9	a
August	23.9 $\pm$ 1.4	b	21.3 $\pm$ 1.4	bc	27.2 $\pm$ 4.1	a	34.1 $\pm$ 4.0	a	48.9 $\pm$ 4.9	ab	44.6 $\pm$ 4.9	ab
October	22.2 $\pm$ 2.7	bc	16.0 $\pm$ 1.8	c	36.3 $\pm$ 3.2	a	30.3 $\pm$ 4.8	a	41.5 $\pm$ 2.3	ab	53.7 $\pm$ 4.9	b
<b><i>ANOVA results</i></b>												
$O_3$	ns		ns		ns							
Month	***		ns		*							
$O_3 \times$ Month	**		ns		ns							

## Supplementary materials

### Interactive effect of leaf age and ozone on mesophyll conductance in Siebold's beech

Yasutomo Hoshika<sup>1\*</sup>, Matthew Haworth<sup>2</sup>, Makoto Watanabe<sup>3</sup> and Takayoshi Koike<sup>4</sup>

*1. Institute of Research on Terrestrial Ecosystems (IRET), National Research Council of Italy (CNR), Via Madonna del Piano, I-50019 Sesto Fiorentino, Italy*

*2. Institute of Sustainable Plant Protection (IPSP), National Research Council of Italy (CNR), Via Madonna del Piano, I-50019 Sesto Fiorentino, Italy*

*3. Institute of Agriculture, Tokyo University of Agriculture and Technology, Fuchu 183-8509, Japan*

*4. Research Faculty of Agriculture, Hokkaido University, Sapporo 060-8689, Japan*

\*Corresponding author:

Yasutomo Hoshika, Tel: +39-055-522-5949, Fax: +39-055-522-5920

E-mail: yasutomo.hoshika@cnr.it

Supplementary figures

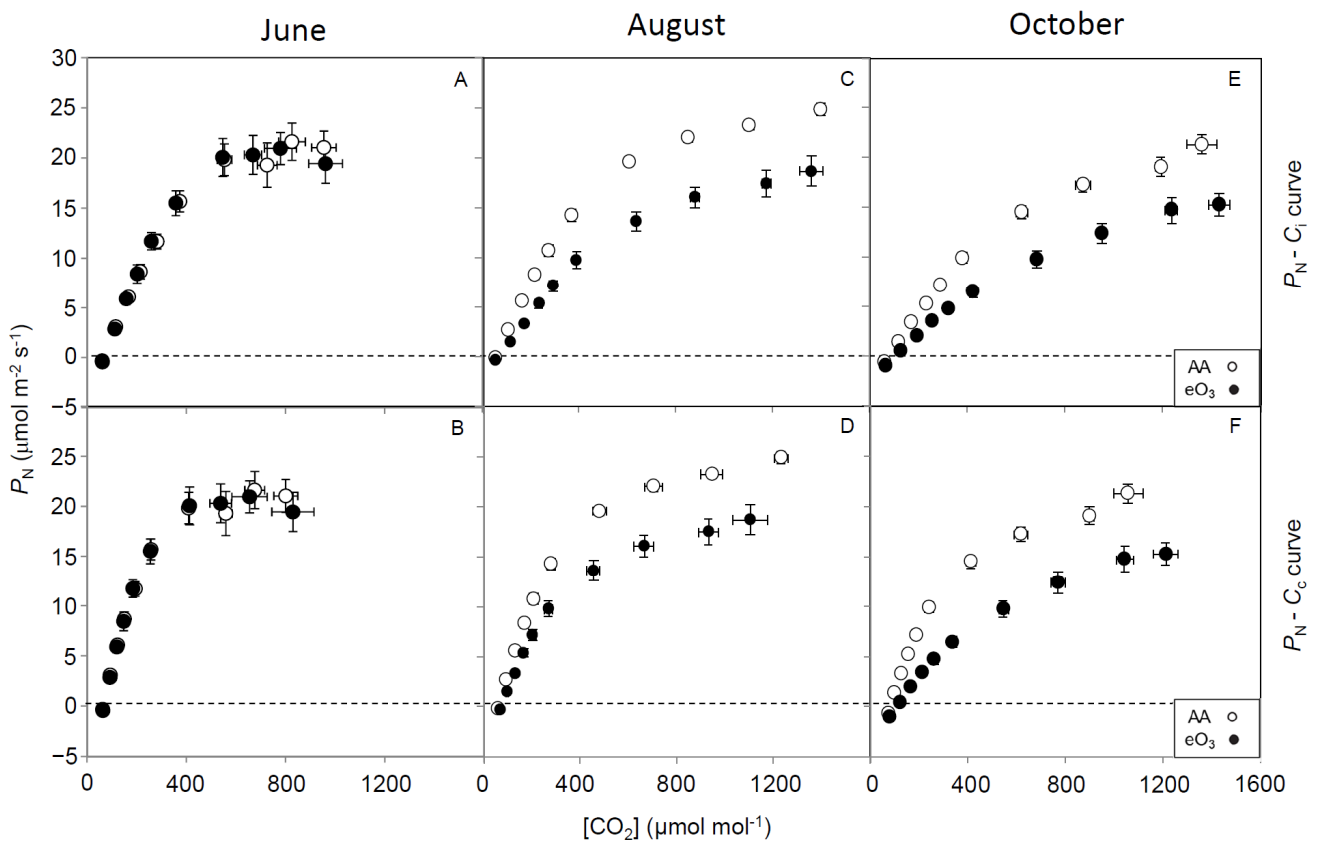


Figure S1. Responses of net photosynthetic rate ( $P_N$ ) to the sub-stomatal concentration of  $CO_2$  ( $C_i$ ) (upper figures) or the concentration of  $CO_2$  inside the chloroplast envelope ( $C_c$ ) (bottom figures) at different ages. The  $P_N/C_i$  curves were obtained by measuring  $P_N$  over 12 ambient  $CO_2$  concentration steps ( $C_a$ , 380, 300, 220, 140, 60, 300, 380, 500, 800, 1100, 1400, 1700  $\mu\text{mol mol}^{-1}$ ). Values of  $G_m$  derived from the curve fitting method (Ethier and Livingston, 2004) were used to calculate the  $P_N/C_c$  curves. Each value is the mean  $\pm$  standard error ( $n = 6$ ).

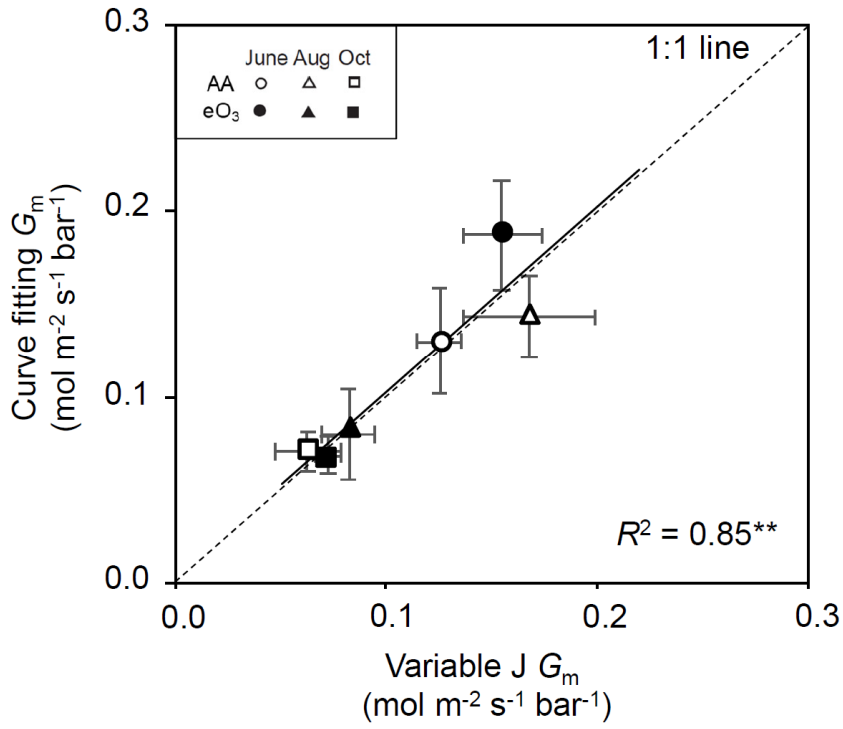


Figure S2. Relationship between mesophyll conductance ( $G_m$ ) values derived from the variable J method and those derived from the  $P_N/C_i$  curve fitting method in Siebold's beech exposed to different  $O_3$  concentrations (ambient [AA] or elevated  $O_3$  [eO<sub>3</sub>]). Each value is the mean  $\pm$  standard error (n = 6). A linear regression analysis: \*\*  $p < 0.01$ .

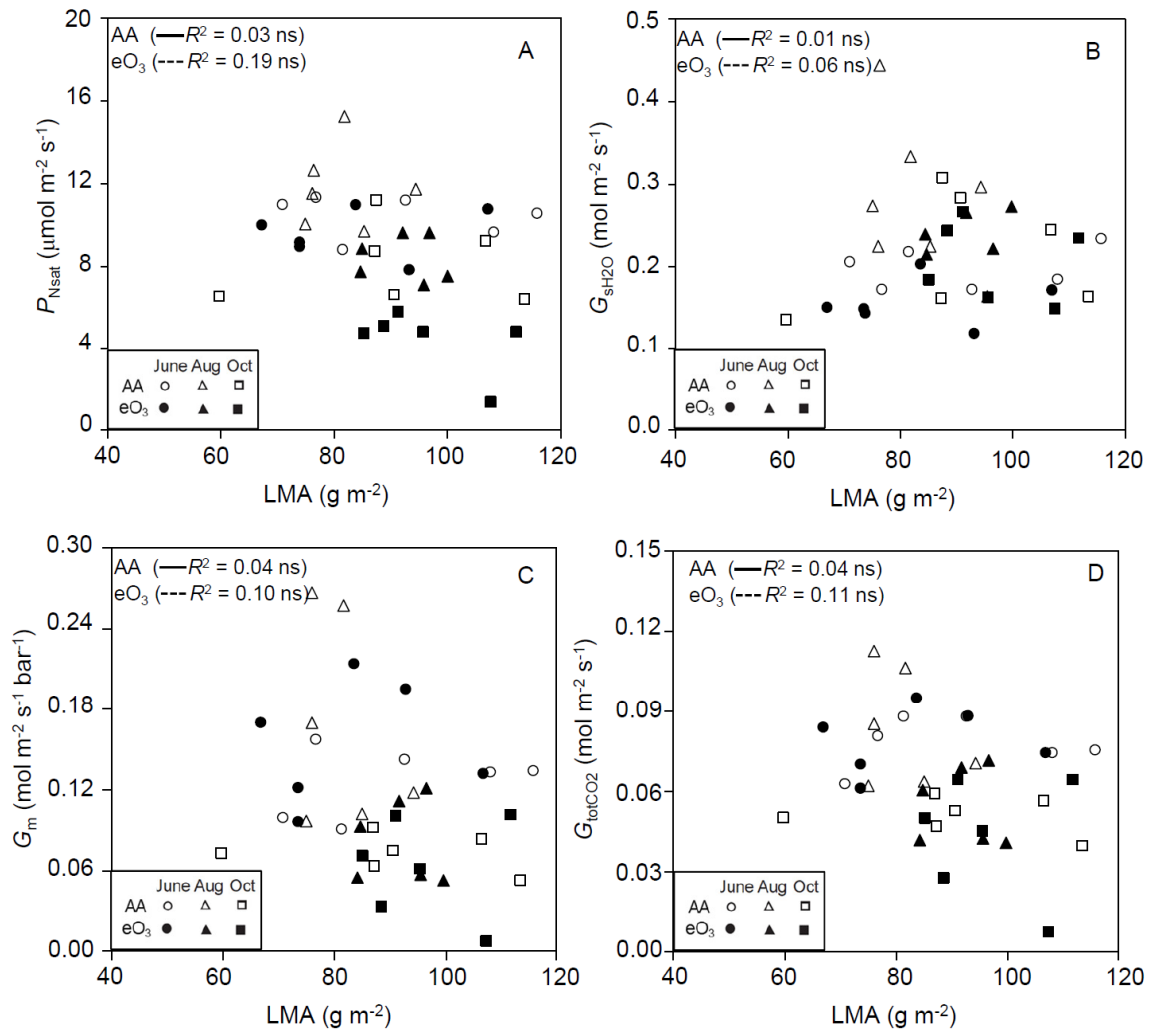


Figure S3. Relationships between leaf gas exchange parameters (A: light-saturated net photosynthetic rate [ $P_{Nsat}$ ], B: stomatal conductance [ $G_{sH_2O}$ ], C: mesophyll conductance [ $G_m$ ] and D: total conductance to CO<sub>2</sub> [ $G_{totCO_2}$ ]) and leaf mass per area (LMA) of Siebold's beech saplings under different O<sub>3</sub> concentrations (ambient [AA] or elevated O<sub>3</sub> [eO<sub>3</sub>]). Simple linear regression analysis was applied to assess the relationships. ns denotes not significant.

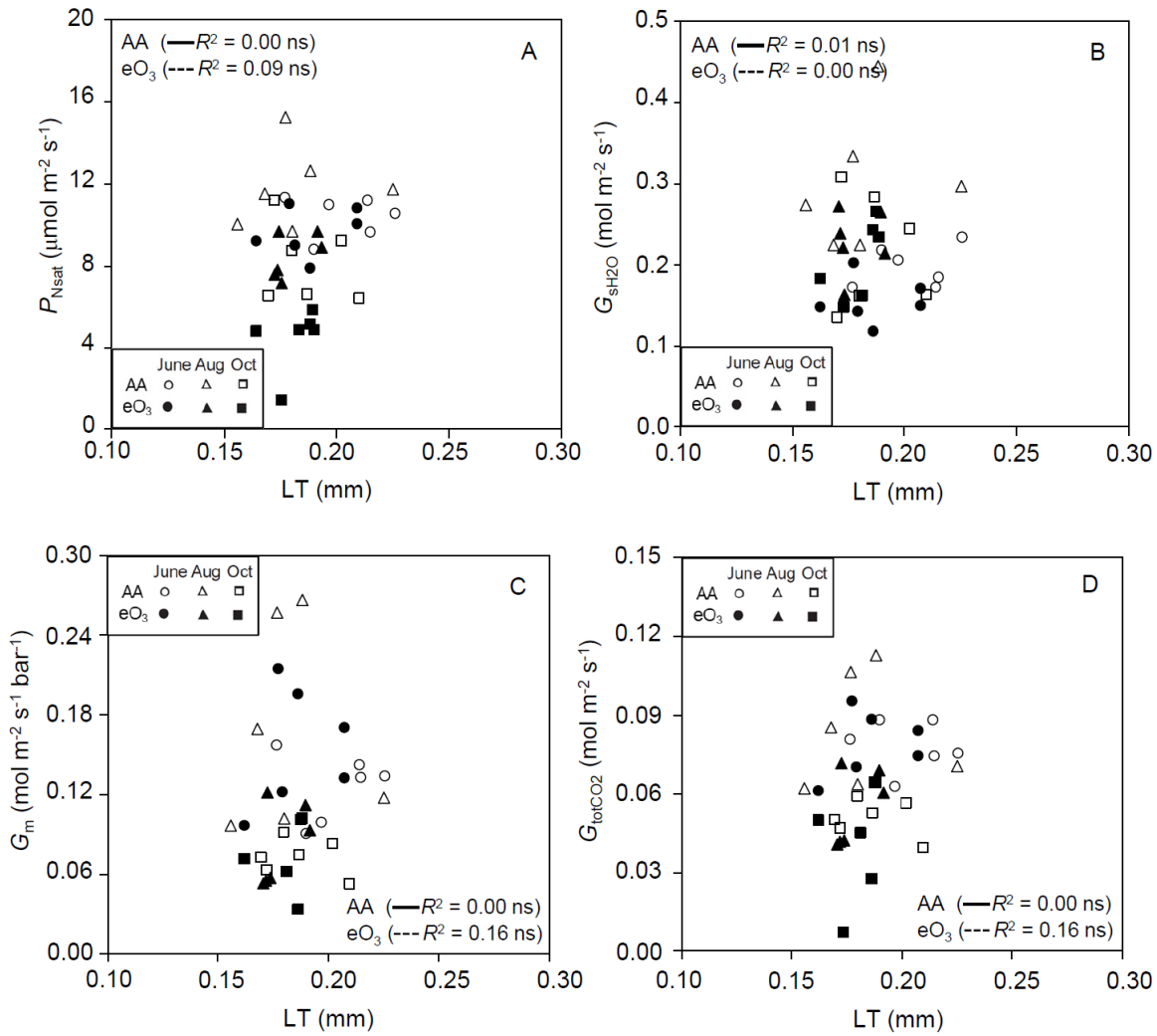


Figure S4. Relationships between leaf gas exchange parameters (A: light-saturated net photosynthetic rate [ $P_{Nsat}$ ], B: stomatal conductance [ $G_{sH_2O}$ ], C: mesophyll conductance [ $G_m$ ] and D: total conductance to  $CO_2$  [ $G_{totCO_2}$ ]) and leaf thickness (LT) of Siebold's beech saplings under different  $O_3$  concentrations (ambient [AA] or elevated  $O_3$  [ $eO_3$ ]). Simple linear regression analysis was applied to assess the relationships. ns denotes not significant.